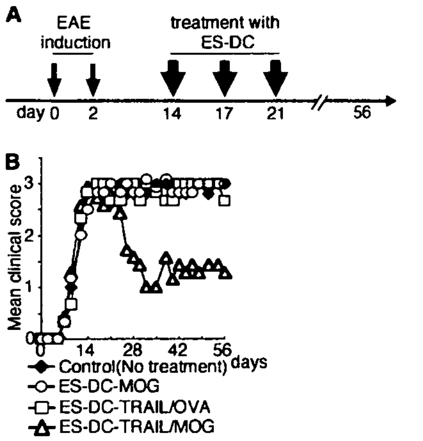

FIGURE 2. Inhibition of MBP-induced EAE by treating the mice with ES-DC-TRAIL/MOG. *A*, The schedule for induction of EAE and treatment is shown. CBF_1 mice (five to seven mice per group) were immunized on days 0 and 2 according to the EAE-induction schedule described above, and subsequently i.p. injected with ES-DC (1×10^6 cells/mouse/injection) on days 14, 17, and 21. *B*, The disease severity of mice immunized with MBP whole protein is shown.

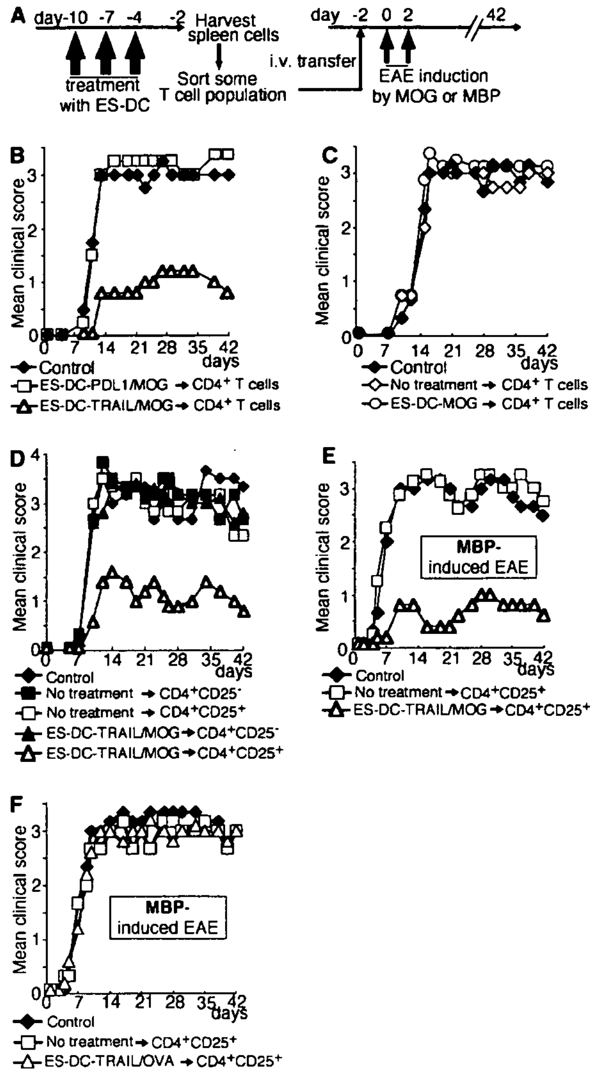

FIGURE 3. Protection from MOG or MBP-induced EAE by the adoptive transfer of $CD4^+CD25^+$ T cells from the mice treated with ES-DC expressing MOG plus TRAIL. *A*, The schedule for the treatment of donor mice with ES-DC, the adoptive transfer of some population of T cells, and the induction of EAE in the recipient mice are shown. The donor CBF_1 mice were i.p. injected with ES-DC (1×10^6 cells/mouse/injection) on days −10, −7, and −4. The T cells were isolated from the donor mice and then transferred to naive mice on day −2. The recipient mice were immunized with MOG peptide (*B–D*) or MBP whole protein (*E* and *F*) on days 0 and 2 according to the EAE-induction protocol as shown in Fig. 1. *B* and *C*, The disease severity of the mice transferred with $CD4^+$ T cells (2.5×10^6 cells/mouse) from ES-DC-TRAIL/MOG, ES-DC-PD-L1/MOG, ES-DC-MOG, ES-DC-TRAIL/OVA-treated mice, or naive mice is shown. *D–F*, The disease severity of the mice transferred with $CD4^+CD25^+$ T cells or $CD4^+CD25^-$ T cells (3×10^5 or 2.2×10^6 cells/mouse, respectively) from ES-DC-TRAIL/MOG-treated mice or naive mice is shown. Control mice were injected with RPMI 1640 medium alone without T cells. The data of all experiments are summarized in Table II.

hind-limb paralysis; 4, complete hind-limb paralysis; 5, fore-limb paralysis or moribundity; 6, death.

Adoptive transfer of T cells

For the adoptive transfer experiments, donor CBF_1 mice were i.p. injected with ES-DC (1×10^6 cells/injection/mouse) on days −10, −7, and −4. $CD4^+$ T cells and $CD4^+CD25^+$ T cells were isolated from the spleen cells of donor mice using the MACS cell sorting system (Miltenyi Biotec). For the isolation of $CD4^+$ T cells, non-$CD4^+$ T cells magnetically labeled with a biotin-conjugated Ab mixture (anti-CD8α, anti-CD11b, anti-CD45R, anti-DX5, and anti-Ter-119) and anti-biotin microbeads were depleted on an autoMACS cell separator. Subsequently, $CD25^+$ T cells, labeled with anti-CD25 mAb conjugated with PE and anti-PE microbeads, were isolated from the $CD4^+$ T cell fraction using positive sorting columns. Cell purity was checked by FACS analysis: $CD4^+$ T cells were >95% after the first step and $CD4^+CD25^+$ cells were >95% after the second step. The $CD4^+$ T cells, $CD4^+CD25^+$ T cells, or $CD4^+CD25^-$ T cells were i.v. injected into recipient mice (2.5×10^6, 3×10^5, or 2.2×10^6 cells/mouse, respectively) on day −2. The recipient mice were subjected to EAE induction (on days 0 and 2) as described above.

Proliferation assay of Treg

Mouse $CD4^+CD25^+$ Treg were purified with a Treg separation kit (MACS) from the spleen cells of naive CBF_1 mice as described above. Assay for the proliferation of Treg was done, as described previously (17). In brief, 1×10^4 ES-DC or syngeneic splenic macrophages were x-ray irradiated (25 Gy), and cocultured with 1×10^4 Treg in the presence of anti-CD3 mAb (clone 145-2C11, 1 μg/ml) and human IL-2 (10–30 U/ml) in wells of 96-well round-bottom culture plates. In some assay, anti-TRAIL mAb (clone N2B2 (5 μg/ml); eBioscience) was added. Splenic macrophages were prepared by collecting plastic dish-adherent cells. The cells were cultured for 3 days, and [^{3}H]thymidine (6.7 Ci/mM) was added to the culture (1 μCi/well) in the last 12 h. At the end of culture, cells were harvested onto glass fiber filters (Wallac) and the incorporation of [^{3}H]thymidine was measured by scintillation counting. The expression of TRAIL in LPS-stimulated spleen cells and macrophages was confirmed by RT-PCR, as described previously (1). The relative quantity of cDNA in each sample was first normalized by PCR for G3PDH. The primer sequences were as follows: TRAIL, 5′-AACCCTCTAGACCGCCGCCACCATGCCTTCCTCAGGGG CCCTGAA-3′ and 5′-GAAATGGTGTCCTGAAAGGTTC; G3PDH, 5′-GG AAAGCTGTGGCGTGATG-3′ and 5′-CTGTTGCTGTAGCCGTATTC-3′.

Immunohistochemical analysis

Freshly excised spinal cords were immediately frozen and embedded in Tissue-Tek OCT compound (Sakura Fine Technical). Immunohistochemical staining of Foxp3 and CD4 was done, as previously described (1, 12), but with some modification. In brief, serial 7-μm sections were made using cryostat and underwent immunochemical staining with anti-Foxp3 mAb (clone FJK-16s, rat IgG2a; eBioscience) or CD4 (clone L3T4; BD Pharmingen), and N-Histofine Simple Stain Mouse MAX PO (Nichirei).

Statistical analysis

The two-tailed Student's *t* test was used to determine any statistical significance of differences. A value of $p < 0.05$ was considered to indicate statistical significance (15). The values indicated in tables are rounded off to the first decimal place.

Table II. *Suppression of EAE induction by adoptive transfer of T cells from CBF_1 mice treated with ES-DC expressing MOG plus TRAIL*[a]

Treatment (ES-DC) of Donor Mice	T Cells Transferred	EAE Induction	Disease Incidence	Day of Onset	Mean Peak Clinical Score
	No transfer	MOG pep	14/14	10.3 ± 1.3	3.6 ± 0.4
TRAIL/MOG	$CD4^+$	MOG pep	3/7	12.3 ± 0.9	1.0 ± 1.1
PD-L1/MOG	$CD4^+$	MOG pep	4/4	10.5 ± 0.8	3.4 ± 0.2
MOG	$CD4^+$	MOG pep	4/4	11.3 ± 1.9	3.4 ± 0.4
No treatment	$CD4^+$	MOG pep	4/4	11.3 ± 1.9	3.0 ± 0.0
TRAIL/MOG	$CD4^+CD25^+$	MOG pep	5/7	14.4 ± 4.2	1.7 ± 1.0
TRAIL/MOG	$CD4^+CD25^-$	MOG pep	7/7	9.0 ± 1.1	3.4 ± 0.2
No treatment	$CD4^+CD25^+$	MOG pep	3/3	9.0 ± 1.3	3.7 ± 0.2
No treatment	$CD4^+CD25^-$	MOG pep	3/3	9.0 ± 1.3	3.8 ± 0.2
	No transfer	MBP pep	18/18	6.4 ± 1.3	3.1 ± 0.1
TRAIL/MOG	$CD4^+CD25^+$	MBP pep	3/8	13.0 ± 8.7	0.8 ± 0.9
TRAIL/OVA	$CD4^+CD25^+$	MBP pep	8/8	6.1 ± 1.4	3.1 ± 0.2
No treatment	$CD4^+CD25^+$	MBP pep	7/7	5.7 ± 1.1	3.1 ± 0.1

[a] The data are combined from a total of 10 separate experiments, including those shown in Fig. 3. The values of onset day and mean peak clinical score are rounded off to the first decimal place.

Results

Prevention of MBP-induced EAE by the transfer of ES-DC genetically engineered to express MOG peptide along with TRAIL

We recently demonstrated the prevention of MOG-induced EAE by treatment with ES-DC expressing MOG peptide plus TRAIL (ES-DC-TRAIL/MOG) or MOG peptide plus PD-L1 (ES-DC-PDL1/MOG). Regarding the mechanism for preventing EAE by the genetically modified ES-DC, we considered not only the possibility of the direct down-modulation of MOG-reactive effector T cells such as the induction of anergy or apoptosis, but also the possibility of promoting MOG-reactive T cells with regulatory or immune-suppressive functions. We hypothesized that, if the latter had been the case, then pretreatment with ES-DC-TRAIL/MOG or ES-DC-PDL1/MOG may thus have had some preventive effect on not only MOG- but also MBP-induced EAE. To test this possibility, we pretreated mice with ES-DC-TRAIL/MOG or ES-DC-PDL1/MOG and subjected them to EAE induction by immunization with MBP (whole protein) or MBP p35-47, according to the schedule depicted in Fig. 1*A*. As a result, we found the severity of both MBP whole protein- and peptide-induced EAE to be significantly reduced by pretreatment with ES-DC-TRAIL/MOG. In contrast, pretreatment with ES-DC-PDL1/MOG, ES-DC-TRAIL/OVA (as irrelevant Ag), and ES-DC-MOG had no effect on MBP-induced EAE (Fig. 1, *B–D*, and Table I).

Next, we tested whether treatment with ES-DC after the onset of MBP-induced EAE would achieve some suppressive effect on the course of disease. The mice immunized according to the protocol for MBP-induced EAE were injected with ES-DC on days 14, 17, and 21 (1×10^6 cells/mouse/injection) as shown in Fig. 2*A*. Even in this postonset treatment, injection of ES-DC-TRAIL/MOG reduced severity of the disease, while ES-DC-TRAIL/OVA and ES-DC-MOG did not do so (Fig. 2*B*).

Prevention of MOG- and MBP-induced EAE by the adoptive transfer of $CD4^+CD25^+$ T cells from the mice treated with ES-DC-TRAIL/MOG

We considered the possibility that MOG-reactive T cells possessing some immunoregulatory effect were activated or propagated by the transferred ES-DC-TRAIL/MOG and that the T cells exerted a protective effect against MBP-induced EAE. To address this possibility, we performed adoptive transfer experiments. We isolated $CD4^+$ T cells from the spleens of the donor mice treated with ES-DC and transferred them into naive recipient mice. Subsequently, the recipient mice were subjected to an immunization procedure for MOG-induced EAE (Fig. 3*A*). As shown in Fig. 3, *B* and *C*, and Table II, the transfer of 2.5×10^6 $CD4^+$ T cells isolated from the mice treated with ES-DC-TRAIL/MOG significantly reduced the severity of EAE of the recipient mice. In contrast, $CD4^+$ T cells isolated from the mice treated with ES-DC-PDL1/MOG or ES-DC-MOG or those from untreated mice showed no effect. These results support the notion that $CD4^+$ T cells with some regulatory activity were induced, activated, or propagated by the treatment with ES-DC-TRAIL/MOG.

Several types of $CD4^+$ T cells with a potential for reducing the severity of Th1 cell-mediated autoimmune diseases are known, such as T regulatory type 1 (Tr1) cells, Th2 cells, or $CD4^+CD25^+$ Treg. To identify the type of T cells involved in the disease-preventive effect, we separated $CD4^+$ T cells isolated from ES-DC-TRAIL/MOG-treated mice into $CD4^+CD25^+$ and $CD4^+CD25^-$ T cells before transfer. In CBF_1 mice, 10–15% of splenic $CD4^+$ T cells were $CD25^+$ (data not shown), thus indicating that 2.5×10^6 $CD4^+$ T cells include $\sim 3 \times 10^5$ $CD25^+$ T cells and 2.2×10^6 $CD25^-$ T cells. Therefore, we transferred 3×10^5 $CD25^+$ T cells and 2.2×10^6 $CD25^-$ T cells into separate mice. As shown in Fig. 3*D* and Table II, the transfer of 3×10^5 $CD4^+CD25^+$ T cells isolated from mice treated with ES-DC-TRAIL/MOG significantly reduced the severity of MOG-induced EAE in the recipient mice. In contrast, the transfer of $CD4^+CD25^+$ or $CD4^+CD25^-$ T cells from naive mice or $CD4^+CD25^-$ T cells from ES-DC-TRAIL/MOG-treated mice had no effect. These results indicate that $CD25^+$ T cells among the $CD4^+$ T cells were responsible for the above-described protective effect of ES-DC-TRAIL/MOG against EAE.

We next tested whether the transfer of $CD4^+CD25^+$ T cells isolated from donor mice treated with ES-DC-TRAIL/MOG would have any effect on MBP-induced EAE. We transferred $CD4^+CD25^+$ T cells from the donor mice treated with ES-DC as described above. Subsequently, the recipient mice were subjected to an immunization procedure for MBP-induced EAE. As shown in Fig. 3, *E* and *F*, and Table II, the transfer of 3×10^5 $CD4^+CD25^+$ T cells isolated from mice treated with ES-DC-TRAIL/MOG significantly reduced the severity of MBP-induced EAE in the recipient mice, but the transfer of $CD4^+CD25^+$ T cells isolated from ES-DC-TRAIL/OVA-treated mice or naive mice did not do so. These results indicate that ES-DC-TRAIL/MOG-

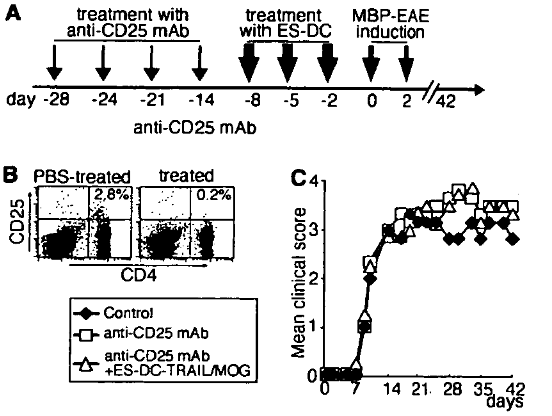

FIGURE 4. The depletion of CD4$^+$CD25$^+$ T cells diminished the preventive effect of ES-DC-TRAIL/MOG on MBP-induced EAE. *A*, The schedule for the depletion with anti-CD25 mAb, pretreatments with ES-DC, and induction of EAE are shown. CBF$_1$ mice (three to four mice per group) were i.p. injected with anti-mouse CD25 mAb (400 μg/mouse/injection) on days -28, -24, -21, -14 and then were treated with ES-DC (1×10^6 cells/mouse/injection) on days -8, -5, and -2. EAE was induced by immunization with MBP whole protein on days 0 and 2 as in Fig. 1. *B*, CD4$^+$CD25$^+$ cells of peripheral blood of anti-CD25 mAb-treated (*right*) and PBS-treated control (*left*) mice were analyzed by flow cytometry on day -2. The percentage of CD4$^+$CD25$^+$ cells among CD4$^+$ cells is shown. *C*, The severity of MBP-induced EAE is shown. Control mice were injected with PBS alone without Ab and RPMI 1640 medium alone without ES-DC. The data of all experiments are summarized in Table I.

induced CD4$^+$CD25$^+$ T cells had a protective effect against not only MOG- but also MBP-induced EAE.

Protection from MBP-induced EAE by ES-DC-TRAIL/MOG depends on CD25$^+$ cells

To further verify the involvement of CD4$^+$CD25$^+$ T cells in the disease-preventive effect of ES-DC-TRAIL/MOG, we performed depletion experiments of CD4$^+$CD25$^+$ T cells. We injected the mice with anti-mouse CD25 mAb four times on days -28, -24, -21, and -14 (Fig. 4*A*). Depletion of CD4$^+$CD25$^+$ T cells was confirmed by flow cytometry analysis of PBLs. CD25$^+$ cells were $0.3 \pm 0.1\%$ of CD4$^+$ T cells in anti-CD25 mAb-treated mice ($n = 4$), whereas they were $2.6 \pm 0.3\%$ in control (PBS-injected) mice ($n = 3$). Representative results of flow cytometry analysis are shown in Fig. 4*B*. Thereafter, we treated the mice with ES-DC-TRAIL/MOG and then immunized them with MBP according to the EAE induction protocol. As shown in Fig. 4*C* and Table I, the effect of ES-DC-TRAIL/MOG to prevent MBP-induced EAE completely disappeared in the mice in which the CD4$^+$CD25$^+$ T cells were depleted. These results further support the possibility that the prevention of MBP-induced EAE by ES-DC-TRAIL/MOG was mediated by CD4$^+$CD25$^+$ T cells. In addition, treatment with anti-CD25 mAb slightly worsened the disease course even when mice were not treated with ES-DC, suggesting that CD4$^+$CD25$^+$ T cells ameliorate the disease to some extent in the natural course after EAE induction.

Increased number of Foxp3$^+$ cells infiltrating into spinal cords of mice treated with ES-DC-TRAIL/MOG

At present, Foxp3 is the most reliable molecular marker for Treg (18). We performed immunohistochemical analysis to detect Foxp3$^+$ cells in the spinal cord of mice treated with ES-DC. We treated the mice with ES-DC and then immunized them with MOG according to the EAE induction protocol. On day 11, the spinal cords harvested from mice were stained with anti-Foxp3 mAb (Fig. 5, *A–C*) and anti-CD4 mAb, and Foxp3$^+$ cells and CD4$^+$ cells were counted. As shown in Fig. 5*D*, the infiltration of Foxp3$^+$ cells into the spinal cord was enhanced in mice treated with ES-DC-TRAIL/MOG, compared with mice with no treatment or mice treated with ES-DC-PDL1/MOG. In contrast, the infiltration of CD4$^+$ cells into the spinal cords was reduced in mice treated with ES-DC-TRAIL/MOG or ES-DC-PDL1/MOG, compared with the observation in mice with no treatment. These results further support the notion of involvement of Treg in the disease-protection effect.

Enhanced capacity of ES-DC expressing TRAIL to induce the in vitro proliferation of naive CD4$^+$CD25$^+$ Tregs

Recent studies have demonstrated that bone marrow-derived DC and splenic DC have a potent capacity to promote the proliferation of CD4$^+$CD25$^+$ Treg both in vitro and in vivo (17, 19). We investigated whether ES-DC had the capacity to promote the proliferation of CD4$^+$CD25$^+$ Treg and also whether the expression of TRAIL had any effect on this capacity of ES-DC. Treg isolated from spleen of naive CBF$_1$ mice were cocultured with ES-DC in the presence of anti-CD3 mAb (1 μg/ml) and a low dose of human IL-2 (10 U/ml). As shown in Fig. 6*A*, all three types of ES-DC, nontransfectant ES-DC, ES-DC-TRAIL, or ES-DC-PDL1, induced a proliferation of Treg more potently than splenic macrophages. The increased proliferation of Treg was observed upon coculture with ES-DC-TRAIL, in comparison to that with other

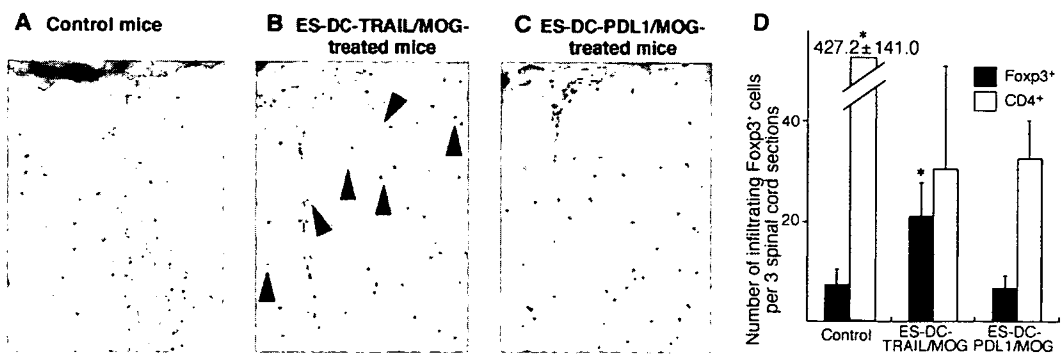

FIGURE 5. Increased number of Foxp3$^+$ cells in spinal cords of mice treated with ES-DC expressing MOG plus TRAIL. CBF$_1$ mice (five mice per group) were pretreated with ES-DC-TRAIL/MOG or PDL1/MOG (1×10^6 cells/mouse/injection) as in Fig. 1 or left untreated. Subsequently, EAE was induced by immunization with MOG peptide on days 0 and 2. The cervical, thoracic, and lumbar spinal cord was isolated on day 11 and subjected to immunohistochemical analysis. The Foxp3$^+$ cells (*A–C*, arrowhead) and CD4$^+$ cells were stained and microscopically counted in three sections of spinal cord (*D*). Results are expressed as mean of samples obtained from five mice ± SD. *, The increase in number of infiltrated cells is statistically significant ($p < 0.01$) as compared with other groups.

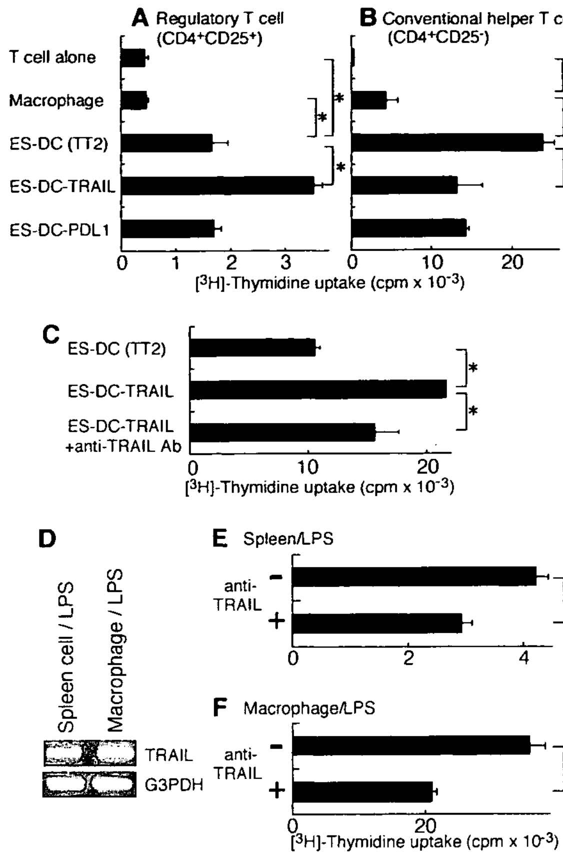

FIGURE 6. Enhanced capacity of APC expressing TRAIL to induce the proliferation of naive $CD4^+CD25^+$ Tregs in vitro. *A*, $CD4^+CD25^+$ T cells (1×10^4) or (*B*) $CD4^+CD25^-$ T cells (1×10^4) isolated from the spleen of the naive CBF_1 mice were cultured alone or cocultured with irradiated stimulators (1×10^4), syngeneic splenic macrophages, nontransfectant ES-DC (TT2), ES-DC-TRAIL, or ES-DC-PDL1, for 3 days in the presence of anti-CD3 mAb (0.1 μg/ml) and human IL-2 (10 U/ml). *C*, $CD4^+CD25^+$ T cells (1×10^4) isolated from the spleen of the naive CBF_1 mice were cultured alone or cocultured with irradiated stimulators (1×10^4), nontransfectant ES-DC (TT2), or ES-DC-TRAIL, for 3 days in the presence of anti-CD3 mAb (2.5 μg/ml) and human IL-2 (10 U/ml) with or without anti-mouse TRAIL mAb (2.5 μg/ml). *D*, The expression of TRAIL in spleen cells or macrophages stimulated with LPS was confirmed by RT-PCR. The naive Treg isolated from a spleen were cocultured for 3 days with 1×10^5 of irradiated LPS-stimulated spleen cells (*E*) or 1×10^4 of irradiated LPS-stimulated macrophages (*F*) in the presence of anti-CD3 mAb (1 μg/ml) and IL-2 (30–100 U/ml) with or without anti-mouse TRAIL mAb (5 μg/ml) for 3 days. The proliferation of responder T cells was quantified by measuring the [^{3}H]thymidine incorporation in the last 12 h of the culture. *, Statistical significance ($p < 0.01$). The results were expressed as the mean of a triplicate assay ± SD. The data are each representative of more than three independent experiments with similar results.

type of ES-DC. In contrast, the magnitude of proliferation of $CD4^+CD25^-$ conventional Th cells was decreased by the expression of TRAIL by ES-DC (Fig. 6*B*). In addition, anti-TRAIL blocking mAb decreased the proliferation of Treg cocultured with ES-DC-TRAIL (Fig. 6*C*). These results suggest that TRAIL expressed on ES-DC has an inhibitory effect on the proliferation of conventional $CD4^+$ T cells and a stimulating effect on that of $CD4^+CD25^+$ Treg.

Anti-TRAIL blocking mAb decreased the proliferation of $CD4^+CD25^+$ Treg responding to LPS-treated natural APCs

The data presented so far suggest that TRAIL expressed on ES-DC has an effect to augment proliferation of $CD4^+CD25^+$ Treg. Lastly, we investigate the effect of TRAIL expressed on natural APCs on proliferation of Treg. Recent studies reported that LPS-stimulation enhanced the expression of TRAIL on spleen cells and bone marrow-derived DC (20–22). We thus examined the proliferation of Treg cocultured with LPS-stimulated whole spleen cells or splenic macrophages in the presence or absence of anti-TRAIL-blocking mAb. Treg isolated from spleen of naive CBF_1 mice were cocultured with LPS-treated APC in the presence of anti-CD3 mAb and a low dose of human IL-2 with or without anti-TRAIL mAb (5 μg/ml). As shown in Fig. 6, *D–F*, anti-TRAIL mAb partially decreased the proliferation of $CD4^+CD25^+$ Treg. These results indicate that TRAIL naturally expressed on APC as well as that expressed on genetically modified ES-DC has a stimulating effect on proliferation of $CD4^+CD25^+$ Treg.

Discussion

In the present study, we found that the severity of not only MOG- but also MBP-induced EAE was reduced by treatment with ES-DC expressing MOG peptide along with TRAIL (Figs. 1 and 2). We obtained several lines of evidences suggesting a possibility that the observed disease-preventive effect is mediated by propagation of MOG-reactive Treg by ES-DC-TRAIL/MOG. Another possible explanation for this phenomenon may be as follows: MOG-reactive T cells might be activated by so-called epitope spreading even in MBP-induced EAE and they might play a major role in the pathogenesis; pretreatment with ES-DC-TRAIL/MOG may abrogate MOG-reactive T cells, thus resulting in a reduction of the disease severity. However, we consider this possibility to be less likely because ES-DC-PDL1/MOG, which showed a MOG-induced EAE-preventive effect similar to that induced by ES-DC-TRAIL/MOG, had no effect on MBP-induced EAE (Fig. 1, *B* and *C*, and Table I). In addition, in previous studies of EAE, the autoreactivity directed to multiple myelin Ags caused by epitope spreading have been observed in chronic or relapsing phases over 4 wk after the immunization. In contrast, the inhibitory effect on MBP-induced EAE, which we observed in the present study, occurred within 2 wk after the immunization. We therefore considered the possibility that MOG-specific T cells with some regulatory activity may have been induced or stimulated by ES-DC-TRAIL/MOG. The results of adoptive transfer experiments demonstrating that $CD4^+$ T cells isolated from ES-DC-TRAIL/MOG-treated donor mice acted to protect the recipient mice from EAE (Fig. 3, *A–C*, and Table II) strongly support this notion.

So far, several types of T cells involved in the negative regulation of immune responses have been identified, such as IL-10-producing Tr1 cells and $CD4^+CD25^+$ Treg (17, 19, 23). Kohm et al. (24) reported that the adoptive transfer of relatively large number of $CD4^+CD25^+$ Treg (2×10^6) isolated from naive mice protected the recipient mice from MOG-induced EAE. It was recently reported that immature DC induced Tr1 cells producing high amounts of IL-10 (25), and also that the proliferation of $CD4^+CD25^+$ Treg was efficiently promoted by DC (17). We thus attempted to characterize the T cells with regulatory activity induced by ES-DC expressing TRAIL and involved in the protection from EAE. We quantified IL-10, IFN-γ, and IL-4 produced by spleen cells isolated from ES-DC-treated mice upon in vitro stimulation with MOG peptide, by ELISA. No significant change in the amount of these cytokines produced by spleen cells of ES-DC-TRAIL/MOG, ES-DC-PDL1/MOG, or ES-DC-MOG-treated mice was observed (data not shown). We thus considered it less likely that the disease-prevention effect was mediated by IL-10-producing Tr1 cells or Th2 cells, although we cannot totally rule out this possibility.

We next assessed the possibility that ES-DC-TRAIL/MOG had propagated or activated $CD4^+CD25^+$ Treg in vivo. Adoptive transfer experiments showed the presence of $CD4^+CD25^+$ T cells with a capacity to prevent not only MOG- but also MBP-induced EAE in ES-DC-TRAIL/MOG-treated mice (Fig. 3, *D–F*, and Table II). In addition, when $CD4^+CD25^+$ T cells were depleted by the pretreatment of mice with anti-CD25 mAb, the protective effect of ES-DC-TRAIL/MOG against MBP-induced EAE was totally abrogated (Fig. 4 and Table I), the observation further supporting the notion that $CD4^+CD25^+$ T cells play a role in the prevention of MBP-induced EAE by treatment with ES-DC-TRAIL/MOG. Recently, Kohm et al. (26) reported that the effect of anti-CD25 Ab is not the depletion but functional inactivation of Treg. Our findings that preventive effect of MBP-induced EAE with ES-DC-TRAIL/MOG was diminished by the injection of anti-CD25 mAb into mice also may be interpreted as inactivation of Treg. Several groups recently reported that $CD4^+CD25^-$ T cells converted to Treg functionality in particular condition (27, 28). It is possible that $CD4^+CD25^+$ Tregs suppressing EAE observed in our study were also those converted from conventional $CD4^+$ T cells.

Furthermore, we observed an increased number of $Foxp3^+$ cells and the ratio of $Foxp3^+$ cells to $CD4^+$ cells in the spinal cords in mice treated with ES-DC-TRAIL/MOG (Fig. 5). In contrast, we could not detect any significant increase in the expression of Foxp3 mRNA in the spleen of ES-DC-TRAIL/MOG-treated mice (data not shown). Also in flow cytometry analysis the proportion of $Foxp3^+$ cells to $CD4^+$ cells in the spleen and inguinal lymph nodes was not increased in mice treated with ES-DC-TRAIL/MOG as compared with control mice (the proportion of $Foxp3^+$ cells to $CD4^+$ cells was 9.7 ± 0.7% in spleen of control mice, 9.8 ± 0.8% in spleen of ES-DC-TRAIL/MOG-treated mice, 9.2 ± 0.9% in inguinal lymph nodes of control mice, and 9.5 ± 0.1% in inguinal lymph nodes of ES-DC-TRAIL/MOG-treated mice). Probably the increase in the number of MOG-reactive $Foxp3^+$ cells was too small to be detected in total $CD4^+$ T cells of spleen and inguinal lymph nodes. In addition, to investigate whether the ES-DC-TRAIL/MOG were acting at the level of priming or within the target organ (CNS), we tested the primary proliferative response to MBP of the T cells of mice treated with ES-DC-TRAIL/MOG before immunization with MBP for EAE induction (as shown in Fig. 1*A*). The inguinal lymph node cells were harvested on day 19 after the immunization and cultured in the presence of MBP (whole protein, 0, 12.5, 25, 50 μg/ml) for 3 days. In this experiment, the treatment with ES-DC-TRAIL/MOG did not reduce the proliferative response to MBP of T cells in inguinal lymph node (data not shown). This result suggests that treatment with ES-DC-TRAIL/MOG did not act at the level of priming. It may be more likely that the treatment with ES-DC-TRAIL/MOG acted in the target organ (CNS), as shown in Fig. 7.

The $CD4^+CD25^+$ T cells induced by ES-DC-TRAIL/MOG and responsible for disease prevention were probably specific to MOG, because ES-DC expressing TRAIL along with irrelevant Ag (OVA) had no effect on MBP-induced EAE (Figs. 1*D* and 3*F* and Tables I and II).

Consistent with recent reports on the stimulation of $CD4^+CD25^+$ Treg as well as conventional T cells by splenic or BM-derived DC (17, 29), in vitro experiments showed that ES-DC also have the capacity to induce proliferation of both $CD4^+CD25^-$ conventional T cells and $CD4^+CD25^+$ Treg, when stimulated with anti-CD3 mAb in the presence of low-dose IL-2. The expression of TRAIL on ES-DC enhanced the capacity to induce proliferation of $CD4^+CD25^+$ Treg, but not of $CD4^+CD25^-$ conventional T cells (Fig. 6, *A* and *B*). In addition, anti-TRAIL-blocking mAb decreased the proliferation of Treg cocultured with ES-DC-TRAIL or natural APC, such as LPS-treated spleen cells or macrophage (Fig. 6, *C–F*). The results of these in vitro experiments suggest that the in vivo transfer of ES-DC-TRAIL/MOG induced proliferation of MOG-reactive Treg which protected the recipient mice from EAE.

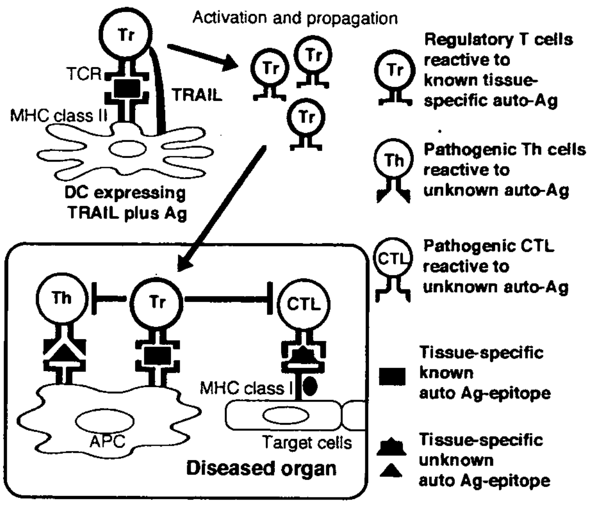

FIGURE 7. Promotion of Tregs with DC expressing TRAIL plus certain tissue-specific autoantigen as a novel strategy for the treatment of the organ-specific autoimmune diseases. DC expressing TRAIL and simultaneously presenting known tissue-specific autoantigen (auto-Ag) in the context of their MHC class II can activate or propagate T cells with a regulatory function (Tr cells) reactive to the autoantigen. In the focus of autoimmune disease, the promoted-Tr cells were retriggered by the same autoantigen expressed in the tissue. Then, the Tr cells inhibited the pathogenic T cells responding to unknown autoantigen. This strategy is applicable, even if target autoantigens are unidentified or if multiple Ags are recognized as targets by the pathogenic autoreactive T cells.

Based on the results obtained in the current study, we consider that the inhibition of autoimmunity by TRAIL-expressing ES-DC may be attributed to the promotion of $CD4^+CD25^+$ T cells by TRAIL, in addition to the induction of apoptosis of pathogenic T cells as suggested by our previous study (1). Mi et al. (30) reported that TRAIL inhibited the proliferation of diabetogenic T cells isolated from NOD mice by suppressing IL-2 production and up-regulating the expression of $p27^{kip1}$. It may be possible that the effects of Treg were involved in their observations. In addition, Herbeuval et al. (31) reported that a level of TRAIL was elevated in plasma of HIV-1-infected patients and in vitro exposure to HIV-1 induced the expression of TRAIL in APCs. Andersson et al. (32) reported expression of Foxp3 to be enhanced in the lymphoid tissue of HIV-infected patients. These two findings may also be related to our findings.

DC modified by some way to enhance their tolerogenic characteristics is regarded as a promising therapeutic means to negatively manipulate the immune response for the treatment of autoimmune and allergic diseases and also for the induction of transplantation tolerance (1, 23, 33–36). In the clinically manifest phase of autoimmune diseases, such as multiple sclerosis or type I diabetes, it is presumed that multiple tissue-specific Ags are recognized as targets by deregulated immunity due to epitope spreading (37). As a result, the induction of a mere deletion or anergy of pathogenic T cells specific to primarily recognized autoantigens may not be sufficient to control these diseases. The promotion of the immune-suppressive T cells reactive to organ-specific self Ags by treatment with genetically modified DC may be a promising therapeutic modality for subjects with autoimmune diseases (Fig. 7). This strategy may also be useful for the induction of transplantation tolerance.

Acknowledgments

We thank Dr. S. Aizawa (RIKEN Center for Developmental Biology, Kobe, Japan) for TT2, Drs. N. Takakura (Kanazawa University, Kanazawa, Japan) and T. Suda (Keio University, Tokyo, Japan) for OP9, Dr. H. Niwa (RIKEN Center for Developmental Biology, Kobe, Japan) for pCAG-IPuro, Drs. T. Okazaki and T. Honjo (Kyoto University, Kyoto, Japan) for a cDNA clone for PD-L1, and Drs. T. Koda and T. Nishimura (Hokkaido University, Sapporo, Japan) for a cDNA clone for OVA.

Disclosures

The authors have no financial conflict of interest.

References

1. Hirata, S., S. Senju, H. Matsuyoshi, D. Fukuma, Y. Uemura, and Y. Nishimura. 2005. Prevention of experimental autoimmune encephalomyelitis by transfer of embryonic stem cell-derived dendritic cells expressing myelin oligodendrocyte glycoprotein peptide along with TRAIL or programmed death-1 ligand. *J. Immunol.* 174: 1888–1897.
2. Wiley, S. R., K. Schooley, P. J. Smolak, W. S. Din, C. P. Huang, J. K. Nicholl, G. R. Sutherland, T. D. Smith, C. Rauch, C. A. Smith, et al. 1995. Identification and characterization of a new member of the TNF family that induces apoptosis. *Immunity* 3: 673–682.
3. Kayagaki, N., N. Yamaguchi, M. Nakayama, K. Takeda, H. Akiba, H. Tsutsui, H. Okamura, K. Nakanishi, K. Okumura, and H. Yagita. 1999. Expression and function of TNF-related apoptosis-inducing ligand on murine activated NK cells. *J. Immunol.* 163: 1906–1913.
4. Nieda, M., A. Nicol, Y. Koezuka, A. Kikuchi, N. Lapteva, Y. Tanaka, K. Tokunaga, K. Suzuki, N. Kayagaki, H. Yagita, et al. 2001. TRAIL expression by activated human $CD4^+V\alpha$ 24NKT cells induces in vitro and in vivo apoptosis of human acute myeloid leukemia cells. *Blood* 97: 2067–2074.
5. Raftery, M. J., M. Schwab, S. M. Eibert, Y. Samstag, H. Walczak, and G. Schonrich. 2001. Targeting the function of mature dendritic cells by human cytomegalovirus: a multilayered viral defense strategy. *Immunity* 15: 997–1009.
6. Hilliard, B., A. Wilmen, C. Seidel, T. S. Liu, R. Goke, and Y. Chen. 2001. Roles of TNF-related apoptosis-inducing ligand in experimental autoimmune encephalomyelitis. *J. Immunol.* 166: 1314–1319.
7. Lamhamedi-Cherradi, S. E., S. J. Zheng, K. A. Maguschak, J. Peschon, and Y. H. Chen. 2003. Defective thymocyte apoptosis and accelerated autoimmune diseases in $TRAIL^{-/-}$ mice. *Nat. Immunol.* 4: 255–260.
8. Song, K., Y. Chen, R. Goke, A. Wilmen, C. Seidel, A. Goke, and B. Hilliard. 2000. Tumor necrosis factor-related apoptosis-inducing ligand (TRAIL) is an inhibitor of autoimmune inflammation and cell cycle progression. *J. Exp. Med.* 191: 1095–1104.
9. Lunemann, J. D., S. Waiczies, S. Ehrlich, U. Wendling, B. Seeger, T. Kamradt, and F. Zipp. 2002. Death ligand TRAIL induces no apoptosis but inhibits activation of human (auto)antigen-specific T cells. *J. Immunol.* 168: 4881–4888.
10. Senju, S., S. Hirata, H. Matsuyoshi, M. Masuda, Y. Uemura, K. Araki, K. Yamamura, and Y. Nishimura. 2003. Generation and genetic modification of dendritic cells derived from mouse embryonic stem cells. *Blood* 101: 3501–3508.
11. Matsuyoshi, H., S. Senju, S. Hirata, Y. Yoshitake, Y. Uemura, and Y. Nishimura. 2004. Enhanced priming of antigen-specific CTLs in vivo by embryonic stem cell-derived dendritic cells expressing chemokine along with antigenic protein: application to antitumor vaccination. *J. Immunol.* 172: 776–786.
12. Motomura, Y., S. Senju, T. Nakatsura, H. Matsuyoshi, S. Hirata, M. Monji, H. Komori, D. Fukuma, H. Baba, and Y. Nishimura. 2006. Embryonic stem cell-derived dendritic cells expressing glypican-3, a recently identified oncofetal antigen, induce protective immunity against highly metastatic mouse melanoma, B16-F10. *Cancer Res.* 66: 2414–2422.
13. Fukuma, D., H. Matsuyoshi, S. Hirata, A. Kurisaki, Y. Motomura, Y. Yoshitake, M. Shinohara, Y. Nishimura, and S. Senju. 2005. Cancer prevention with semi-allogeneic ES cell-derived dendritic cells. *Biochem. Biophys. Res. Commun.* 335: 5–13.
14. Fujii, S., S. Senju, Y. Z. Chen, M. Ando, S. Matsushita, and Y. Nishimura. 1998. The CLIP-substituted invariant chain efficiently targets an antigenic peptide to HLA class II pathway in L cells. *Hum. Immunol.* 59: 607–614.
15. Uemura, Y., S. Senju, K. Maenaka, L. K. Iwai, S. Fujii, H. Tabata, H. Tsukamoto, S. Hirata, Y. Z. Chen, and Y. Nishimura. 2003. Systematic analysis of the combinatorial nature of epitopes recognized by TCR leads to identification of mimicry epitopes for glutamic acid decarboxylase 65-specific TCRs. *J. Immunol.* 170: 947–960.
16. Morgan, M. E., R. P. Sutmuller, H. J. Witteveen, L. M. van Duivenvoorde, E. Zanelli, C. J. Melief, A. Snijders, R. Offringa, R. R. de Vries, and R. E. Toes. 2003. $CD25^+$ cell depletion hastens the onset of severe disease in collagen-induced arthritis. *Arthritis Rheum.* 48: 1452–1460.
17. Yamazaki, S., T. Iyoda, K. Tarbell, K. Olson, K. Velinzon, K. Inaba, and R. M. Steinman. 2003. Direct expansion of functional $CD25^+CD4^+$ regulatory T cells by antigen-processing dendritic cells. *J. Exp. Med.* 198: 235–247.
18. Sakaguchi, S. 2003. The origin of FOXP3-expressing $CD4^+$ regulatory T cells: thymus or periphery. *J. Clin. Invest.* 112: 1310–1312.
19. Walker, L. S., A. Chodos, M. Eggena, H. Dooms, and A. K. Abbas. 2003. Antigen-dependent proliferation of $CD4^+CD25^+$ regulatory T cells in vivo. *J. Exp. Med.* 198: 249–254.
20. Mariani, S. M., and P. H. Krammer. 1998. Surface expression of TRAIL/Apo-2 ligand in activated mouse T and B cells. *Eur. J. Immunol.* 28: 1492–1498.
21. Santini, S. M., C. Lapenta, M. Logozzi, S. Parlato, M. Spada, T. Di Pucchio, and F. Belardelli. 2000. Type I interferon as a powerful adjuvant for monocyte-derived dendritic cell development and activity in vitro and in Hu-PBL-SCID mice. *J. Exp. Med.* 191: 1777–1788.
22. Yu, Y., S. Liu, W. Wang, W. Song, M. Zhang, W. Zhang, Z. Qin, and X. Cao. 2002. Involvement of tumour necrosis factor-α-related apoptosis-inducing ligand in enhanced cytotoxicity of lipopolysaccharide-stimulated dendritic cells to activated T cells. *Immunology* 106: 308–315.
23. Menges, M., S. Rossner, C. Voigtlander, H. Schindler, N. A. Kukutsch, C. Bogdan, K. Erb, G. Schuler, and M. B. Lutz. 2002. Repetitive injections of dendritic cells matured with tumor necrosis factor α induce antigen-specific protection of mice from autoimmunity. *J. Exp. Med.* 195: 15–21.
24. Kohm, A. P., P. A. Carpentier, H. A. Anger, and S. D. Miller. 2002. Cutting edge: $CD4^+CD25^+$ regulatory T cells suppress antigen-specific autoreactive immune responses and central nervous system inflammation during active experimental autoimmune encephalomyelitis. *J. Immunol.* 169: 4712–4716.
25. Wakkach, A., N. Fournier, V. Brun, J. P. Breittmayer, F. Cottrez, and H. Groux. 2003. Characterization of dendritic cells that induce tolerance and T regulatory 1 cell differentiation in vivo. *Immunity* 18: 605–617.
26. Kohm, A. P., J. S. McMahon, J. R. Podojil, W. S. Begolka, M. DeGutes, D. J. Kasprowicz, S. F. Ziegler, and S. D. Miller. 2006. Cutting edge: anti-CD25 monoclonal antibody injection results in the functional inactivation, not depletion, of $CD4^+CD25^+$ T regulatory cells. *J. Immunol* 176: 3301–3305.
27. Liang, S., P. Alard, Y. Zhao, S. Parnell, S. L. Clark, and M. M. Kosiewicz. 2005. Conversion of $CD4^+CD25^-$cells into $CD4^+CD25^+$ regulatory T cells in vivo requires B7 costimulation, but not the thymus. *J. Exp. Med.* 201: 127–137.
28. Chen, W., W. Jin, N. Hardegen, K. J. Lei, L. Li, N. Marinos, G. McGrady, and S. M. Wahl. 2003. Conversion of peripheral $CD4^+CD25^-$naive T cells to $CD4^+CD25^+$ regulatory T cells by TGF-β induction of transcription factor Foxp3. *J. Exp. Med.* 198: 1875–1886.
29. Tarbell, K. V., S. Yamazaki, K. Olson, P. Toy, and R. M. Steinman. 2004. $CD25^+CD4^+$ T cells, expanded with dendritic cells presenting a single autoantigenic peptide, suppress autoimmune diabetes. *J. Exp. Med.* 199: 1467–1477.
30. Mi, Q. S., D. Ly, S. E. Lamhamedi-Cherradi, K. V. Salojin, L. Zhou, M. Grattan, C. Meagher, P. Zucker, Y. H. Chen, J. Nagle, et al. 2003. Blockade of tumor necrosis factor-related apoptosis-inducing ligand exacerbates type 1 diabetes in NOD mice. *Diabetes* 52: 1967–1975.
31. Herbeuval, J. P., A. Boasso, J. C. Grivel, A. W. Hardy, S. A. Anderson, M. J. Dolan, C. Chougnet, J. D. Lifson, and G. M. Shearer. 2005. TNF-related apoptosis-inducing ligand (TRAIL) in HIV-1-infected patients and its in vitro production by antigen-presenting cells. *Blood* 105: 2458–2464.
32. Andersson, J., A. Boasso, J. Nilsson, R. Zhang, N. J. Shire, S. Lindback, G. M. Shearer, and C. A. Chougnet. 2005. Cutting edge: the prevalence of regulatory T cells in lymphoid tissue is correlated with viral load in HIV-infected patients. *J. Immunol.* 174: 3143–3147.
33. Lu, L., and A. W. Thomson. 2002. Manipulation of dendritic cells for tolerance induction in transplantation and autoimmune disease. *Transplantation* 73: S19–S22.
34. Liu, Z., X. Xu, H. C. Hsu, A. Tousson, P. A. Yang, Q. Wu, C. Liu, S. Yu, H. G. Zhang, and J. D. Mountz. 2003. CII-DC-AdTRAIL cell gene therapy inhibits infiltration of CII-reactive T cells and CII-induced arthritis. *J. Clin. Invest.* 112: 1332–1341.
35. Terness, P., T. M. Bauer, L. Rose, C. Dufter, A. Watzlik, H. Simon, and G. Opelz. 2002. Inhibition of allogeneic T cell proliferation by indoleamine 2,3-dioxygenase-expressing dendritic cells: mediation of suppression by tryptophan metabolites. *J. Exp. Med.* 196: 447–457.
36. Sato, K., T. Nakaoka, N. Yamashita, H. Yagita, H. Kawasaki, C. Morimoto, M. Baba, and T. Matsuyama. 2005. TRAIL-transduced dendritic cells protect mice from acute graft-versus-host disease and leukemia relapse. *J. Immunol.* 174: 4025–4033.
37. Vanderlugt, C. L., and S. D. Miller. 2002. Epitope spreading in immune-mediated diseases: implications for immunotherapy. *Nat. Rev. Immunol.* 2: 85–95.

Embryonic Stem Cell–Derived Dendritic Cells Expressing Glypican-3, a Recently Identified Oncofetal Antigen, Induce Protective Immunity against Highly Metastatic Mouse Melanoma, B16-F10

Yutaka Motomura,[1] Satoru Senju,[1] Tetsuya Nakatsura,[1] Hidetake Matsuyoshi,[1] Shinya Hirata,[1] Mikio Monji,[1] Hiroyuki Komori,[1] Daiki Fukuma,[1] Hideo Baba,[2] and Yasuharu Nishimura[1]

Departments of [1]Immunogenetics and [2]Gastroenterological Surgery, Graduate School of Medical Sciences, Kumamoto University, Kumamoto, Japan

Abstract

We have recently established a method to generate dendritic cells from mouse embryonic stem cells. By introducing exogenous genes into embryonic stem cells and subsequently inducing differentiation to dendritic cells (ES-DC), we can now readily generate transfectant ES-DC expressing the transgenes. A previous study revealed that the transfer of genetically modified ES-DC expressing a model antigen, ovalbumin, protected the recipient mice from a challenge with an ovalbumin-expressing tumor. In the present study, we examined the capacity of ES-DC expressing mouse homologue of human glypican-3, a recently identified oncofetal antigen expressed in human melanoma and hepatocellular carcinoma, to elicit protective immunity against glypican-3-expressing mouse tumors. CTLs specific to multiple glypican-3 epitopes were primed by the *in vivo* transfer of glypican-3-transfectant ES-DC (ES-DC-GPC3). The transfer of ES-DC-GPC3 protected the recipient mice from subsequent challenge with B16-F10 melanoma, naturally expressing glypican-3, and with glypican-3-transfectant MCA205 sarcoma. The treatment with ES-DC-GPC3 was also highly effective against i.v. injected B16-F10. No harmful side effects, such as autoimmunity, were observed for these treatments. The depletion experiments and immunohistochemical analyses suggest that both CD8$^+$ and CD4$^+$ T cells contributed to the observed antitumor effect. In conclusion, the usefulness of glypican-3 as a target antigen for antimelanoma immunotherapy was thus shown in the mouse model using the ES-DC system. Human dendritic cells expressing glypican-3 would be a promising means for therapy of melanoma and hepatocellular carcinoma. (Cancer Res 2006; 66(4): 2414-22)

Introduction

To establish effective immunotherapy for cancer, it is absolutely imperative to identify ideal tumor-specific antigens as targets of antitumor immunotherapy. In addition, the development of the methods to direct immune responses toward the antigens is essential. The manipulation of dendritic cells, specialized antigen-presenting cells, is one of the promising strategies to improve the efficacy of immunotherapy for cancer (1). Currently, numerous reports have shown that dendritic cells loaded with dead tumor cells, tumor cell lysates, tumor antigenic proteins, or peptides can induce immunity and clinical responses (2–5). However, these vaccines often induce a weak immune response that is insufficient for clinical therapy because many tumor antigens are self-antigens against which the immune system has acquired tolerance (6, 7). For loading tumor antigens to dendritic cells for anticancer immunotherapy, the gene-based antigen expression by dendritic cells is considered to be superior to loading antigen as a peptide, protein, or tumor cell lysate (8). For the efficient gene transfer to dendritic cells, the use of virus-based vectors is required because dendritic cells is relatively unsuitable for genetic modification. Clinical trials using dendritic cells genetically modified with virus vectors (e.g., monocyte-derived dendritic cells introduced with adenovirus vectors encoding for tumor antigens) are now under way (9–11). Considering the broader medical applications of this method, the drawbacks of genetic modification with virus vectors include the potential risk accompanying the use of virus vectors and legal restrictions related to it. As a result, the development of safer and more efficient means is considered to be desirable.

We recently established a novel method for the genetic modification of dendritic cells (12). In this method, we generated dendritic cells from mouse embryonic stem cells by *in vitro* differentiation. The levels of expression of MHC molecules and costimulatory molecules, CD80 and CD86, in embryonic stem cell–derived dendritic cells (ES-DC) were comparable with those of bone marrow–derived dendritic cells (BM-DC; ref. 12). The capacity of ES-DC to simulate T cells was comparable with that of dendritic cells generated *in vitro* from BM-DC. We can readily generate genetically modified ES-DC by introducing expression vectors into embryonic stem cells and the subsequent induction of their differentiation into ES-DC (13, 14). The transfection of embryonic stem cells can be done with electroporation using plasmid vectors, and the use of virus-based vectors is not necessary. Once a proper embryonic stem cell transfectant clone is established, it then serves as an infinite source for genetically modified dendritic cells. In a previous study, we showed that the *in vivo* transfer of ES-DC expressing a model tumor antigen, ovalbumin, potently primed ovalbumin-specific CTLs, thereby eliciting a protective effect against ovalbumin-expressing tumor cells (13).

Many of the genes or gene families encoding many cancer/testis antigen or oncofetal antigens have thus far been identified and regarded as ideal targets for anticancer immunotherapy (15–18). However, only a few tumor-associated antigens have been reported as the inducer of both CD8$^+$ and CD4$^+$ T-cell-mediated immune responses (19–22). Recently, we and other groups found that an oncofetal protein glypican-3, glycosylphosphatidylinositol (GPI)–anchored membrane protein, is specifically overexpressed in human

Requests for reprints: Satoru Senju and Yasuharu Nishimura, Department of Immunogenetics, Graduate School of Medical Sciences, Kumamoto University, Kumamoto 860-8556, Japan. Phone: 81-96-373-5313; Fax: 81-96-373-5314; E-mail: senjusat@gpo.kumamoto-u.ac.jp and mxnishim@gpo.kumamoto-u.ac.jp.

doi:10.1158/0008-5472.CAN-05-2090

hepatocellular carcinoma (23, 24). In a subsequent study, we revealed that glypican-3 is overexpressed also in human melanoma (25). An immunohistochemical analysis revealed that the tissue distribution of murine glypican-3 protein was very similar to that in humans. In a previous study, we showed that the *in vivo* transfer of glypican-3 peptide-pulsed BM-DC or glypican-3-reactive CTL line had a potent effect to protect the recipient mice from the murine glypican-3-transfected Colon 26, a colorectal cancer cell line (17).

In the current study, we found that a mouse melanoma cell line F10, which is a subline of B16, naturally expressed glypican-3. Using this cell line as a target, we elucidated the antitumor effect of therapy with ES-DC genetically modified to express murine glypican-3.

Materials and Methods

Mice. CBA and C57BL/6 mice were obtained from Clea Animal Co. (Tokyo, Japan) or Charles River (Hamamatsu, Japan) and maintained under specific pathogen-free conditions. Male CBA and female C57BL/6 mice were mated to produce (CBA × C57BL/6) F1 (CBF1) mice and all studies were done with the F1 mice syngeneic to the mouse embryonic stem cell line TT2 at 6 to 8 weeks of age. The mouse experiments met with approval by Animal Research Committee of Kumamoto University.

Cell lines. The embryonic stem cell line TT2, derived from CBF1 blastocysts (26), was maintained as described previously (12). The method for induction of differentiation *in vitro* of embryonic stem cells into dendritic cells was done as described previously (12), and ES-DC prepared from a 14-day culture in bacteriologic Petri dishes in the presence of granulocyte-macrophage colony-stimulating factor (GM-CSF) were used for *in vivo* and *in vitro* assays. C57BL/6-derived tumor cell lines, F1 and F10 sublines of B16 melanoma, a fibrosarcoma cell line MCA205 (MCA), Lewis lung cancer (3LL) and a thymoma cell line EL4, and a human hepatocellular carcinoma cell line HepG2 were provided by the Cell Resource Center for Biomedical Research Institute of Development, Aging, and Cancer, Tohoku University (Sendai, Japan). The cells were cultured in RPMI 1640 supplemented with 10% FCS. To produce glypican-3-expressing MCA (MCA-GPC3), MCA cells were transfected with pCAGGS-GPC3-internal ribosomal entry site (IRES)-puromycin-resistant (puro-R) by using LipofectAMINE 2000 reagent (Invitrogen Corp., Carlsbad, CA), selected with puromycin, and then subjected to cloning by limiting dilution in drug-free medium using 96-well culture plates (27, 28).

Generation of ES-DC expressing glypican-3. A full-length murine *glypican-3* cDNA clone was purchased from Invitrogen. A cDNA fragment encoding total glypican-3 protein was isolated from that and transferred to a mammalian expression vector pCAGGS-IRES-puro-R, containing the CAG promoter and an IRES-puro-R *N*-acetyltransferase gene cassette (29, 30), to generate an expression vector for *glypican-3*, pCAGGS-GPC3-IRES-puro-R. To generate *glypican-3*-transfected embryonic stem cell clones, TT2 embryonic stem cells were introduced with pCAGGS-GPC3-IRES-puro-R by electroporation and selected with puromycin as described previously (12). *Glypican-3*-transfectant embryonic stem cell clones were subjected to a differentiation culture to generate ES-DC as described previously (12–14). No maturation stimuli, such as lipopolysaccharide or tumor necrosis factor-α, were given to ES-DC before *in vivo* transfer. The expression of *glypican-3* in transfectant ES-DC was confirmed by reverse transcription-PCR (RT-PCR).

RT-PCR and Northern blotting. Total cellular RNA was extracted and RT-PCR was done as described previously (13, 14). Briefly, total RNA was converted into cDNA and PCR was done for 33 cycles for the quantification of *glypican-3* mRNA and for 30 cycles for the quantification of glyceraldehyde-3-phosphate dehydrogenase (*GAPDH*) mRNA. The primer sequences were as follows: *glypican-3*, sense 5′-CTGACTGACCGCGTTAC-TCCCACA-3′ and antisense 5′-TAGCAGCATCGCCACCAGCAAGCA-3′ and *GAPDH*, sense 5′-GGAAAGCTGTGGCGTGATG-3′ and antisense 5′-CTGTT-GCTGTAGCCGTATTC-3′. The sense strand primer used for detection of transgene-derived mRNA was corresponding to the 5′ untranslated region included in the vector DNA. PCR products were visualized by ethidium bromide staining after separation over a 1% agarose gel. A Northern blot analysis was done as described previously (31). In brief, RNA samples (20 μg total RNA per lane) were subjected to electrophoresis in formalin-MOPS gels, blotted onto nylon membranes (Hybond N$^+$, Amersham, Piscataway, NJ), and probed with ^{32}P-labeled DNA probe. A human *glypican-3* cDNA fragment (bp 1,639-2,139) was used as a probe. Human and murine *glypican-3* have a 90% similarity in nucleotide sequence and human cDNA probe hybridized to both human and murine *glypican-3* mRNA.

Peptides, protein, and cytokines. Eleven kinds of 9- to 10-mer glypican-3-derived peptides predicted to bind with H2-D^b or K^b were selected based on the binding score as calculated by the BIMAS software package (BioInformatics and Molecular Analysis Section, Center for Information Technology, NIH, Bethesda, MD). The peptides were synthesized by the F-MOC method on an automatic peptide synthesizer (PSSM8; Shimadzu, Kyoto, Japan) and subsequently purified by high-performance liquid chromatography. The synthetic peptides were designated as murine glypican-3-1 to -11 in ascending order of high binding score. Their amino acid sequences are as follows: murine glypican-3-1, AMFKNNYPSL; murine glypican-3-2, LGSDINVDDM; murine glypican-3-3, LTARINMEQL; murine glypican-3-4, SVLDINECL; murine glypican-3-5, TLCWNGQEL; murine glypican-3-6, YVQKNGGKL; murine glypican-3-7, GMVKVKNQL; murine glypican-3-8, RNGMKNQFNL; murine glypican-3-9, AMLLGLGCL; murine glypican-3-10, ASMELKFLI; and murine glypican-3-11, LFPVIYTQM. Murine glypican-3-11 is predicted to be restricted to H2-K^b and the others to H2-D^b. Recombinant human glypican-3 protein was purchased from R&D Systems (Minneapolis, MN). Recombinant murine GM-CSF and IFN-γ were purchased from PeproTech (London, United Kingdom).

Immunohistochemical and flow cytometric analysis. An immunofluorescence analysis to detect the expression of glypican-3 was done as described previously (16). Anti-human glypican-3 polyclonal antibody was purchased from Santa Cruz Biotechnology (Santa Cruz, CA). FITC-labeled goat anti-rabbit IgG (clone ALI4408; Biosource, Camarillo, CA) was used as a second antibody and propidium iodide for nuclear DNA staining. Stained samples were subjected to microscopic analysis on a confocal microscope (Fluoview FV300, Olympus, Tokyo, Japan). Immunohistochemical analysis of frozen tissue sections was done as described previously (13, 23) using monoclonal antibody (mAb) specific to CD4 (L3T4; BD PharMingen, San Diego, CA) or CD8 (Ly-2; BD PharMingen). In the flow cytometric analysis, cell samples were stained and analyzed on a flow cytometer (FACScan; BD Biosciences, Japan) as described previously (12, 14). Antibodies used for staining were as follows: FITC-conjugated mouse anti-mouse H2-D^b (clone CTDb; mouse IgG2a; Caltag, Burlingame, CA), anti-H2-K^b (clone CTKb; mouse IgG2a; Caltag) and anti-I-A^b (clone 3JP; mouse IgG2a; Caltag), R-phycoerythrin (R-PE)–conjugated anti-mouse CD11c (clone N148; hamster IgG; Chemicon, Temecula, CA), R-PE-conjugated anti-mouse CD86 (clone RMMP-2; rat IgG2a; Caltag), FITC-conjugated goat anti-mouse Ig (BD PharMingen), mouse IgG2a control (clone G155-178; BD PharMingen), FITC-conjugated mouse IgG2a control (clone G155-178; BD PharMingen), and R-PE-conjugated hamster IgG control (Immunotech, Marseille, France).

Generation of BM-DC. Generation of dendritic cells from bone marrow cells was done as described previously (17). For loading of synthetic peptides, BM-DC were incubated with a mixture of three kinds of glypican-3 peptides, murine glypican-3-2, -8, and -11 (10 μmol/L each), at 37°C for 2 hours. For loading of recombinant glypican-3 protein, BM-DC were cultured in the presence of glypican-3 protein (2 μg/mL) at 37°C for 12 hours. No maturation stimuli were given to BM-DC before *in vivo* transfer.

Induction of glypican-3-specific CTLs and cytotoxicity assay. The mice were i.p. immunized with 1×10^5 ES-DC twice with a 7-day interval. Seven days after the second immunization, spleen cells were isolated from the mice and cultured (2.5×10^6 per well) with ES-DC (1×10^5 per well) in 24-well culture plates in RPMI supplemented with 10% horse serum, recombinant human interleukin (IL)-2 (100 units/mL), and 2-mercaptoethanol (50 μmol/L). After the culture for 5 days, the cells were recovered and their cytotoxic activity was analyzed by ^{51}Cr release assays using MCA, MCA-GPC3, B16-F1, and B16-F10 as target cells basically by the same method as described previously (12). B16 cells were pretreated with recombinant murine IFN-γ (1,000 units/mL) before use as target cells as reported previously (32). In some experiments, $CD8^+$ T cells and natural killer (NK) cells were isolated from effector cell preparations by using a magnetic cell sorting system (Miltenyi, Bergisch Gladbach, Germany). Positively selected cells were 95% pure as determined by flow cytometry.

ELISPOT analysis. Glypican-3-specific T cells were induced by a culture of splenocytes isolated from mice immunized with ES-DC-GPC3 by the same way as described above, except that glypican-3-derived peptides (10 μmol/L) were added to the culture instead of ES-DC-GPC3. After 5 days, the frequency of cells producing IFN-γ on stimulation with target cells (EL4 or EL4 pulsed with each peptide, MCA or MCA-GPC3) was assessed by an ELISPOT assay as described previously (33). The spots were automatically counted and subsequently analyzed using the Eliphoto system (Minerva Tech, Tokyo, Japan).

Tumor prevention and treatment. ES-DC-GPC3 or BM-DC (1×10^5) loaded with glypican-3 peptide or protein were transferred i.p. into mice twice on days −14 and −7, and B16-F10 or MCA-GPC3 cells were challenged s.c. into the shaved back region on day 0. The tumor sizes were determined biweekly in a blinded fashion and survival rate or disease free rate was monitored. Tumor index was calculated as follows: tumor index (mm^2) = (length × width). For the i.v. challenge experiments, tumor cells (B16-F10) were injected i.v. on day 0, and 1×10^5 ES-DC-GPC3 were injected i.p. twice on days 3 and 10 as described previously (34).

***In vivo* depletion of $CD4^+$ and $CD8^+$ T cells.** The mice were transferred i.p. twice with 1×10^5 ES-DC-GPC3 on days −14 and −7 and challenged s.c. with 5×10^3 B16-F10 cells on day 0. For the depletion of T-cell subsets *in vivo*, mice were given a total of six i.p. transfers of the ascites (0.1 mL/mouse/transfer) from hybridoma-bearing nude mice or anti-asialo GM1 on days −18, −15, −11, −8, −4, and −1. Antibodies used were rat anti-mouse CD4 mAb (clone GK1.5), rat anti-mouse CD8 mAb (clone 2.43), and rabbit anti-asialo GM1 polyclonal antibody (Wako Japan; 20 μL/mouse/transfer). Normal rat IgG (Sigma-Aldrich, St. Louis, MO; 200 μg/mouse/transfer) was used as a control. The depletion of T-cell subsets by treatment with antibodies was confirmed by a flow cytometric analysis of spleen cells, which showed a >90% specific depletion.

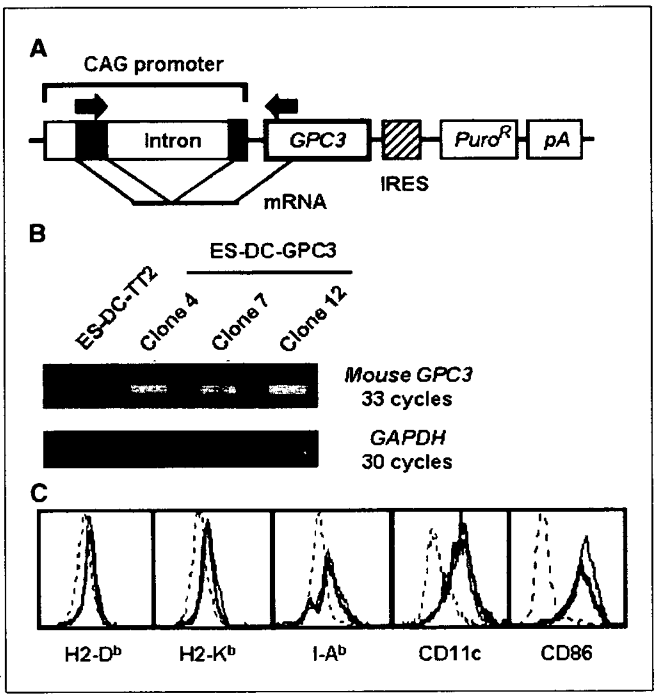

Figure 1. Establishment of ES-DC genetically modified to express murine glypican-3. *A*, structure of pCAGGS-GPC3-IRES-puro-R vector. To obtain pCAGGS-GPC3-IRES-puro-R, a cDNA fragment, including a full-length cDNA of murine *glypican-3*, was inserted into a mammalian expression vector pCAGGS-IRES-puro-R containing the CAG promoter and an IRES-puromycin *N*-acetyltransferase gene cassette. *B*, expression of *glypican-3* mRNA detected by RT-PCR analysis in transfectant ES-DC (ES-DC-GPC3). Primer sets (*arrows* in *A*) were designed to span the intron (917 bp) in the CAG promoter sequence to distinguish PCR products of mRNA origin (249 bp) from the genome-integrated vector DNA origin (1,166 bp). *Black boxes* in (*A*) indicate the 5'-untranslated region of the rabbit β-actin gene included in the CAG promoter. PCR was done at the cycles indicated for quantification of *glypican-3* mRNA and *GAPDH* mRNA. *C*, surface phenotype of genetically modified ES-DC. The expression of the cell surface $H2\text{-}D^b$, $H2\text{-}K^b$, $I\text{-}A^b$, CD11c, and CD86 on transfectant ES-DC was analyzed by a flow cytometric analysis. The staining patterns of ES-DC-GPC3 (*thick line*) closely coincided with those of parental ES-DC (*thin line*). *Dotted lines*, findings for isotype-matched control staining.

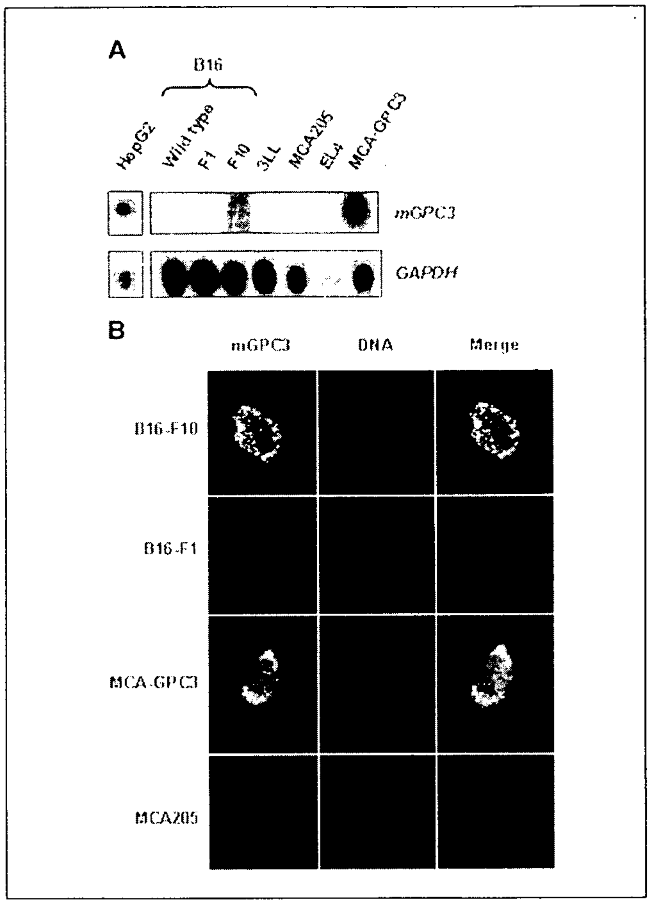

Figure 2. Expression of glypican-3 in cancer cell lines. *A*, Northern blot analysis of *glypican-3* mRNA in a human hepatocellular carcinoma cell line HepG2 (positive control) and various cancer cell lines of C57BL/6 origin. The same filters were stripped and rehybridized with *GAPDH* cDNA to assess the loading of equal amounts of RNA. *B*, immunofluorescence staining analysis of murine glypican-3 protein expressed in B16 variants F1, F10, MCA205, and MCA-GPC3. These cells were stained with rabbit anti-human glypican-3 polyclonal antibody cross-reactive to murine glypican-3 (*green*). Chromosome DNA was visualized by propidium iodide staining (*red*).

Statistical analysis. The two-tailed Student's *t* test was used to determine the statistical significance of differences in the cytolytic activity and tumor growth between the treatment groups. $P < 0.05$ was considered to be significant. The Kaplan-Meier plot for survival was assessed for significance in the tumor challenge experiments using the Breslow-Gehan-Wilcoxon test. Statistical analyses were made using the StatView 5.0 software package (Abacus Concepts, Calabasas, CA).

Results

Generation of ES-DC expressing glypican-3. TT2 embryonic stem cells were introduced with a murine glypican-3 expression vector, pCAGGS-GPC3-IP, driven by the CAG promoter and containing the IRES-puro-R marker gene (Fig. 1A), and several transfectant clones were isolated. The transfectant embryonic stem cell clones were subjected to differentiation to ES-DC, and a transfectant clone 12 expressing the highest level of glypican-3 was selected based on the RT-PCR analysis (Fig. 1B). ES-DC differentiated from parental embryonic stem cell line TT2 without transfection were designated as ES-DC-TT2, and ES-DC differentiated from glypican-3-transfectant embryonic stem cells were designated as ES-DC-GPC3. No significant difference was observed in the morphology and levels of the surface expression of H2-D^b, H2-K^b, I-A^b, CD11c, and CD86 between ES-DC-TT2 and ES-DC-GPC3 (Fig. 1C). As a result, the transfection of the *glypican-3* gene has little influence on the differentiation of ES-DC.

Expression of glypican-3 in a F10 subline of B16 melanoma. We recently revealed that the oncofetal protein glypican-3 is specifically overexpressed in human hepatocellular carcinomas and melanomas (23, 25). To establish a mouse model system to evaluate the glypican-3 as a target antigen for anticancer immunotherapy, we searched for a transplantable mouse tumor cell line naturally expressing glypican-3. We examined the expression of glypican-3 in several mouse cell lines and found that B16-F10, a subline of B16 melanoma, expressed glypican-3. In a Northern blot analysis, as shown in Fig. 2A, where a human hepatocellular carcinoma cell line HepG2 was used as a positive control, *glypican-3* mRNA was evidently detected in a mouse melanoma cell line B16-F10 but not in B16-W.T., B16-F1, 3LL, MCA205, or EL4. The expression of *glypican-3* mRNA was also detected in a glypican-3-transfected MCA, MCA-GPC3. Figure 2B shows an immunofluorescence analysis to detect expression of glypican-3 protein. In accordance with the result of the Northern blot analysis, evident expression of glypican-3 protein was detected in B16-F10 and MCA-GPC3. On the other hand, MCA205 and B16-F1 cells did not express glypican-3 protein. Glypican-3 is a GPI-anchored membrane protein, and the results shown in Fig. 2B indicated that glypican-3 protein localized at or around cell membrane is

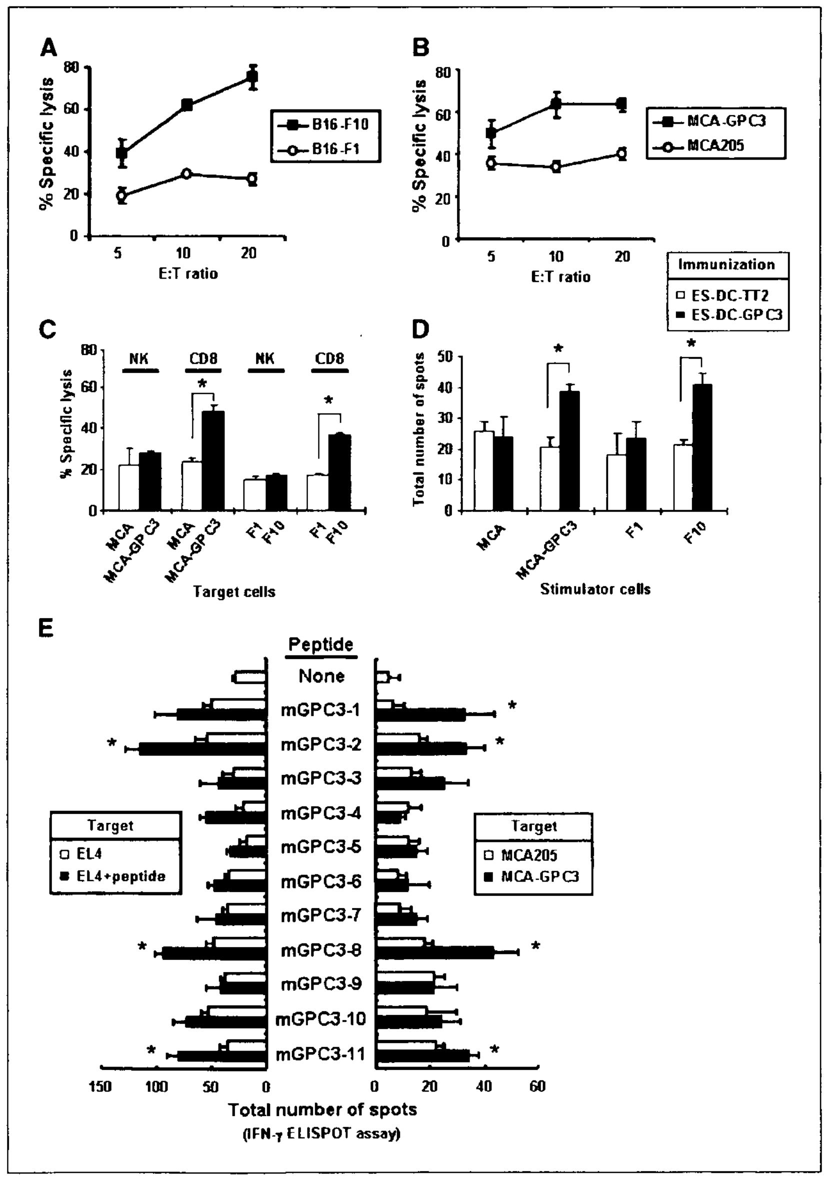

Figure 3. Priming of antigen-specific CTLs with ES-DC-GPC3. The mice were transferred i.p. twice with 1×10^5 ES-DC-GPC3 on days −14 and −7. On day 0, spleen cells from immunized mice were isolated and cultured with 1×10^5 ES-DC-GPC3 per well in the presence of recombinant human IL-2 (100 units/mL) for 5 days. ^{51}Cr release assays were done with the obtained resultant cells to evaluate the capacity to kill IFN-γ pretreated B16-F1 and B16-F10 cells (*A*) and MCA and MCA-GPC3 cells (*B*). Results are expressed as % specific lysis from triplicate assays. *C*, in addition, the resultant cells obtained in the same way were sorted to the fraction of NK cells and CD8$^+$ T cells with microbeads, and another assay was done using the targets in the same condition as in (*A* and *B*). *D*, spleen cells from mice transferred twice with 1×10^5 ES-DC-GPC3 or ES-DC-TT2, respectively, were isolated and restimulated *in vitro* with 1×10^5 ES-DC-GPC3 per well for 5 days. The resultant cells were used for IFN-γ ELISPOT assay. The assay was done in triplicate using the same targets as in (*A* and *B*). *Columns*, mean number of IFN-γ-positive spots. *E*, identification of glypican-3-derived and H2-D^b- or H2-K^b-restricted CTL epitopes by IFN-γ ELISPOT assays. The mice were immunized with 1×10^5 ES-DC-GPC3 twice with a 7-day interval. Spleen cells from mice immunized were restimulated *in vitro* with each glypican-3 peptide (10 μmol/L) and cultured for 5 days with 100 units/mL recombinant human IL-2. ELISPOT assays for 16 hours were examined against EL4 pulsed with or without each peptide and MCA or MCA-GPC3. *Columns*, mean total number of spots from quadruplicate assays. Data are representative of three independent experiments with similar results in (*A-E*). *, $P < 0.05$, differences in the responses are statistically significant between two values in (*C-E*).

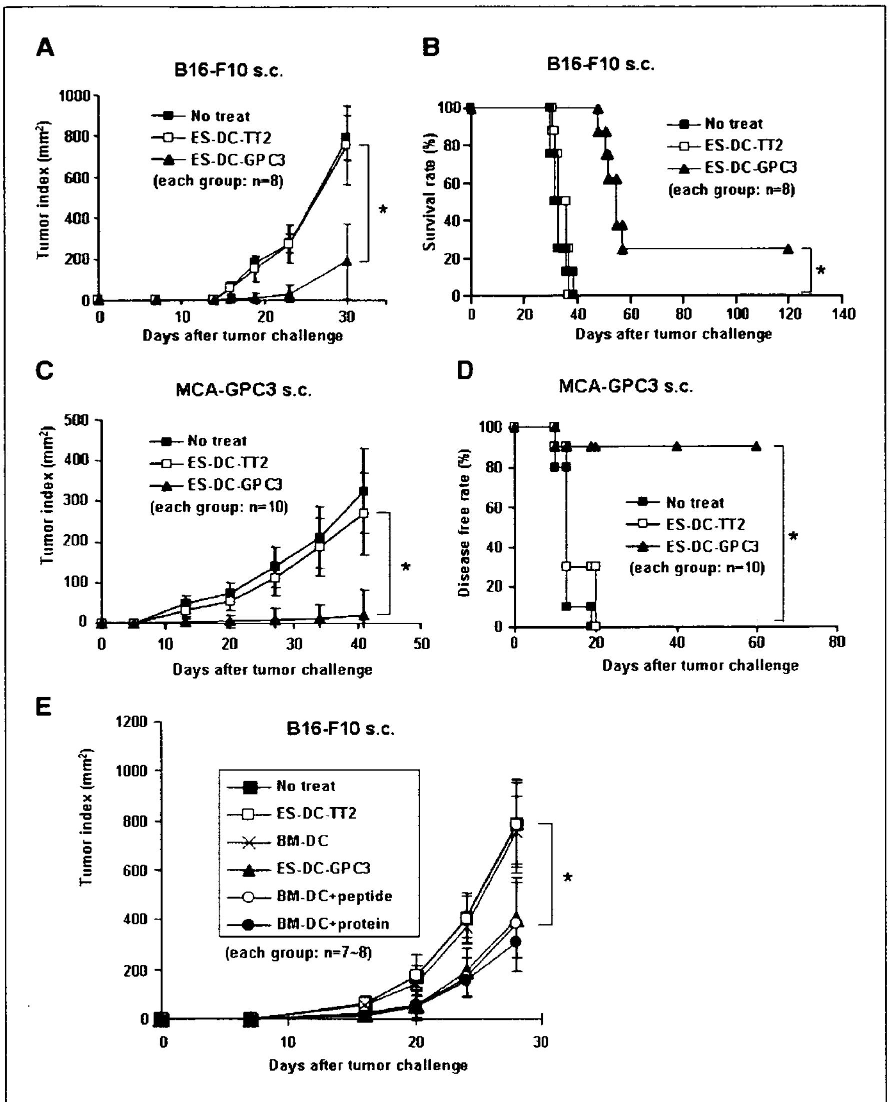

Figure 4. Suppression of tumor growth and prolongation of survival by preimmunization with ES-DC-GPC3. The mice were transferred i.p. twice with 1×10^5 ES-DC-GPC3 or ES-DC-TT2 on days −14 and −7. On day 0, the mice were challenged s.c. with 5×10^3 B16-F10 (*A* and *B*) or 1×10^5 MCA-GPC3 (*C* and *D*) expressing glypican-3. The tumor index, survival rate, or disease-free rate was monitored. *, $P < 0.05$, differences in these three indexes between the groups treated with ES-DC-GPC3 and ES-DC-TT2 were statistically significant. *E,* mice were injected i.p. with ES-DC-GPC3 or BM-DC loaded with a mixture of glypican-3 peptides, murine glypican-3-2, -8, and -11, or glypican-3 protein on the same schedule as in (*A-D*) and challenged s.c. with 5×10^3 B16-F10. Subsequently, the mice were monitored for the growth of tumor.

consistent with this, although some differences in the staining patterns among the cells were observed.

Priming of antigen-specific cytotoxic T cells with genetically modified ES-DC-GPC3. We analyzed the capacity of ES-DC-GPC3 to prime glypican-3-specific CTLs. The mice were immunized i.p. twice with ES-DC-GPC3 or ES-DC-TT2 on days −14 and −7. On day 0, the spleen cells were isolated and restimulated *in vitro* with ES-DC-GPC3 in the presence of exogenous recombinant human IL-2 (100 units/mL). After 5 days, the cells were recovered and their killing activity against target cells with or without expression of glypican-3 was analyzed. As shown in Fig. 3*A* and *B*, the effector cells primed by ES-DC-GPC3 showed a significantly higher killing activity against B16-F10 than against B16-F1, and also against MCA-GPC3 than nontransfectant MCA cells. These results suggest that the effector cells included CTLs recognizing glypican-3. In the experiments shown in Fig. 3*C*, we separated the effector cells into $CD8^+$ T cells and NK cells before the killing assay. NK cells showed activity to kill MCA and MCA-GPC3 in a similar magnitude and to kill B16-F1 and F10 in a similar magnitude, indicating that they killed target cells regardless of glypican-3 expression. On the other hand, for the $CD8^+$ fraction, the cytotoxic activity against B16-F10 was higher than that against B16-F1, and the cytotoxic activity against MCA-GPC3 was higher than that against MCA. On the contrary, spleen cells isolated from mice transferred with ES-DC-TT2 and cocultured *in vitro* with ES-DC-GPC3 exhibited the similar basal levels of killing activities directed against both B16-F1 and F10 as well as MCA and MCA-GPC3 (data not shown).

We next compared the efficiency of the induction of glypican-3-specific and IFN-γ-producing T cells primed by ES-DC-GPC3 with that primed by ES-DC-TT2. The mice were immunized twice with ES-DC-TT2 or ES-DC-GPC3 based on the above described schedule, and the splenocytes isolated from both group of mice were cocultured with ES-DC-GPC3 for 5 days. Thereafter, the frequency of glypican-3-specific T cells was analyzed by an ELISPOT analysis to detect cells producing IFN-γ. As shown in Fig. 3*D*, *in vivo* priming with ES-DC-GPC3 and ES-DC-TT2 resulted in the induction of similar frequency of cells producing IFN-γ on stimulation with cells with no expression of glypican-3, MCA or B16-F1. On the other hand, *in vivo* priming with ES-DC-GPC3 led to the induction of significantly larger number of T cells producing IFN-γ

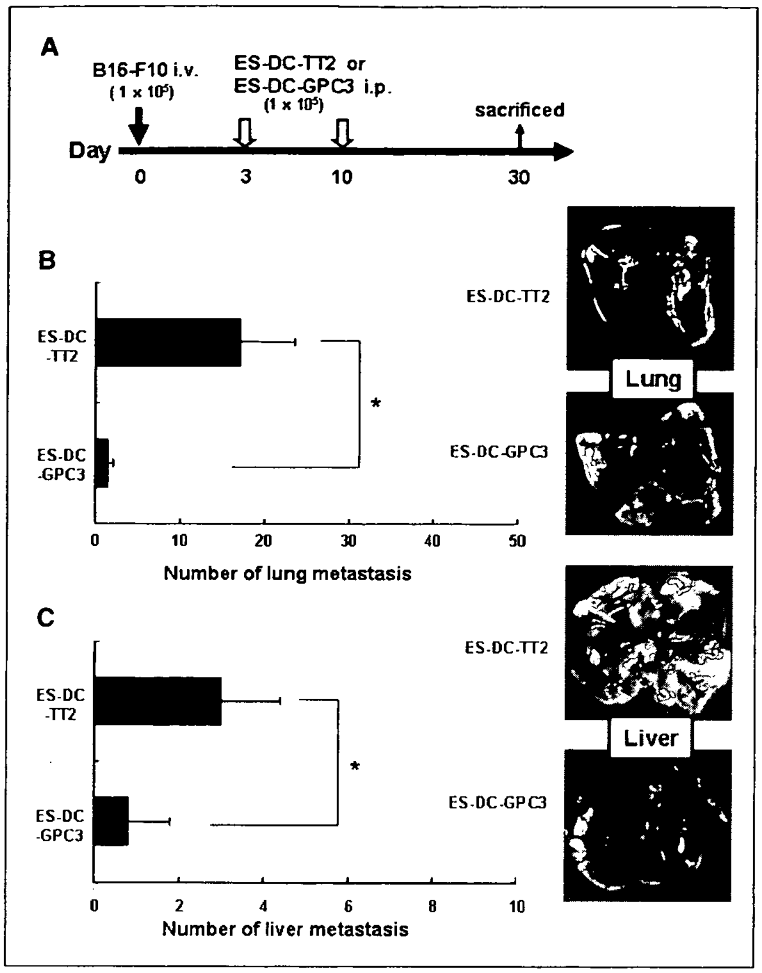

Figure 5. Suppression of tumor growth in the metastatic tumor model of B16-F10. The protocol for therapeutic immunotherapy model was indicated in (*A*). All mice were injected into tail vein with 1×10^5 F10 cells on day 0. On days 3 and 10, mice were injected i.p. with 1×10^5 ES-DC-TT2 or ES-DC-GPC3. On day 30, the mice were sacrificed and the numbers of pulmonary and liver metastases were macroscopically calculated. *Columns,* mean number of total metastases in the lung (*B*) and liver (*C*) using five mice per group. *, $P < 0.05$, differences in the number of metastases are statistically significant between the two values.

on stimulation with cells expressing glypican-3, MCA-GPC3 or B16-F10, compared with priming with ES-DC-TT2. Collectively, these results showed that glypican-3-specific CTLs were primed *in vivo* only when mice were transferred with ES-DC-GPC3, further confirming that ES-DC-GPC3 have the capacity to prime the glypican-3-specific CTLs *in vivo*.

Identification of glypican-3-derived and H2-D^b- or K^b-restricted CTL epitopes. To identify the H-2^b-restricted CTL epitopes of glypican-3, we synthesized 11 glypican-3-derived peptides carrying the binding peptide motifs for H2-D^b or K^b and designated as murine glypican-3-1 to -11 in turn. Spleen cells of the mice immunized with ES-DC-GPC3 by the same procedure as described above were stimulated *in vitro* with each of the peptides instead of ES-DC-GPC3 for 5 days. Subsequently, the frequency of glypican-3-specific CTLs was analyzed by IFN-γ ELISPOT assays. As shown in Fig. 3*E*, cells stimulated *in vitro* with murine glypican-3-2, -8, or -11 showed specific IFN-γ production on restimulation with EL4 cells prepulsed with the same peptide or MCA-GPC3. These results indicate that glypican-3-specific CTLs primed *in vivo* with ES-DC-GPC3 included those recognizing multiple glypican-3 epitopes.

Tumor preventive effects of immunization with ES-DC-GPC3. We next asked whether ES-DC-GPC3 could induce a protective immunity against tumor cells expressing glypican-3 *in vivo*. We immunized mice by the i.p. transfer of ES-DC on days −14 and −7, and the mice were challenged s.c. with 5×10^3 B16-F10 cells or 1×10^5 MCA-GPC3 on day 0. We then monitored the growth of tumors and survival of the mice. As shown in Fig. 4, immunizations with ES-DC-GPC3 provided a significant degree of protection against both B16-F10 and MCA-GPC3. On the other hand, the transfer of ES-DC-TT2 gave no significant protection compared with mice without dendritic cell transfer. Immunization with ES-DC-GPC3 did not show a protective effect against MCA or B16-F1 with no glypican-3 expression (data not shown). Collectively, the *in vivo* administration of ES-DC-GPC3 induced antitumor immunity against glypican-3-expressing tumor cells, thus resulting in a significant inhibition of the growth of tumor and prolongation of the survival time of the treated mice.

Next, we compared ES-DC-GPC3 with BM-DC preloaded with glypican-3 peptide or protein in their capacity to induce antitumor effect. We generated BM-DC from bone marrow cells of CBF1 mice and loaded them with mixture of the three major H2-D^b-restricted epitopes, murine glypican-3-2, -8, and -11 (Fig. 3*E*), or recombinant glypican-3 protein. As shown in Fig. 4*E*, ES-DC-GPC3 and peptide or protein antigen-loaded BM-DC elicited similar magnitude of protective effect against challenge with B16-F10.

Protective effect of ES-DC-GPC3 against i.v. challenge with tumor cells. We next examined the antitumor effect of ES-DC-GPC3 against i.v. challenge with B16-F10. As shown in Fig. 5*A*, the mice were i.v. inoculated with B16-F10 cells on day 0, and the mice were treated with ES-DC-TT2 or ES-DC-GPC3 twice on days 3 and 10. On day 30, mice were sacrificed and macroscopically analyzed. As shown in Fig. 5B and C, treatment with ES-DC-GPC3 significantly reduced the pulmonary and liver metastases in comparison with the treatment with ES-DC-TT2 ($P < 0.05$). Some of the mice treated with ES-DC-TT2, but not those treated with ES-DC-GPC3, died before they were scheduled to be sacrificed. Thus, the survival time of the mice treated with ES-DC-GPC3 was prolonged in comparison with those treated with ES-DC-TT2.

Identification of effector cells involved in the protection against F10 and MCA-GPC3 induced by ES-DC-GPC3. To determine the subsets of the effector cells involved in the observed protective effect against tumor cells induced by ES-DC-GPC3, we depleted $CD4^+$ or $CD8^+$ T cells in the mice by treatments with either anti-CD4 or anti-CD8 mAb. By this treatment, >90% of $CD4^+$ or $CD8^+$ T cells were depleted (data not shown). The NK cells were depleted by the treatment with anti–asialo GM1 antibody. During this procedure, the mice were immunized with ES-DC-GPC3 and challenged s.c. with B16-F10 cells. As shown in Fig. 6, depletion of $CD4^+$ T cells, $CD8^+$ T cells, or NK cells almost totally abrogated the protective immunity induced by ES-DC-GPC3, suggesting that all of three effector cell subsets were essential for the protective effect.

In a histologic analysis of the tumor tissue specimens, we observed more intense infiltration of inflammatory cells into and/or around tumor tissues of mice immunized with ES-DC-GPC3 than those of mice immunized with ES-DC-TT2. In the metastatic B16-F10 tumor tissue specimens, the infiltrating cells were found to consist of both $CD4^+$ and $CD8^+$ T cells (Fig. 6). These results also suggest that both $CD4^+$ and $CD8^+$ T cells were involved in the antitumor effect against the B16-F10 induced by ES-DC-GPC3.

Discussion

We investigated the antitumor effect of immunization with ES-DC genetically engineered to express a mouse oncofetal antigen glypican-3 against mouse tumor cells naturally expressing GPC3-F10, a subline of B16 melanoma. *In vivo* transfer of ES-DC-GPC3 primed CTL reactive to multiple glypican-3-derived epitopes. The treatment of mice with ES-DC-GPC3 elicited potent protective effect against B16-F10 in both preventive and therapeutic conditions with no evidence of any side effects, such as autoimmunity. The antitumor effect induced by ES-DC-GPC3 was specific to the tumor cells expressing glypican-3, because this treatment was not effective against B16-F1, another subline of B16 with no glypican-3 expression. The glypican-3 specificity of the antitumor effect induced by ES-DC-GPC3 was further confirmed by the observation that the treatment was effective against glypican-3-transfectant MCA205 sarcoma but not against parental MCA 205 cells. The depletion experiments and immunohistochemical analyses showed that $CD8^+$ T cells, $CD4^+$ T cells, and NK cells contributed to the observed antitumor effect.

The tumor cell lines used in this study, MCA205 and B16-F10, were derived from C57BL/6 mice and may be recognized by some fraction of NK cells of CBF1 mice. Thus, the tumor cells must be

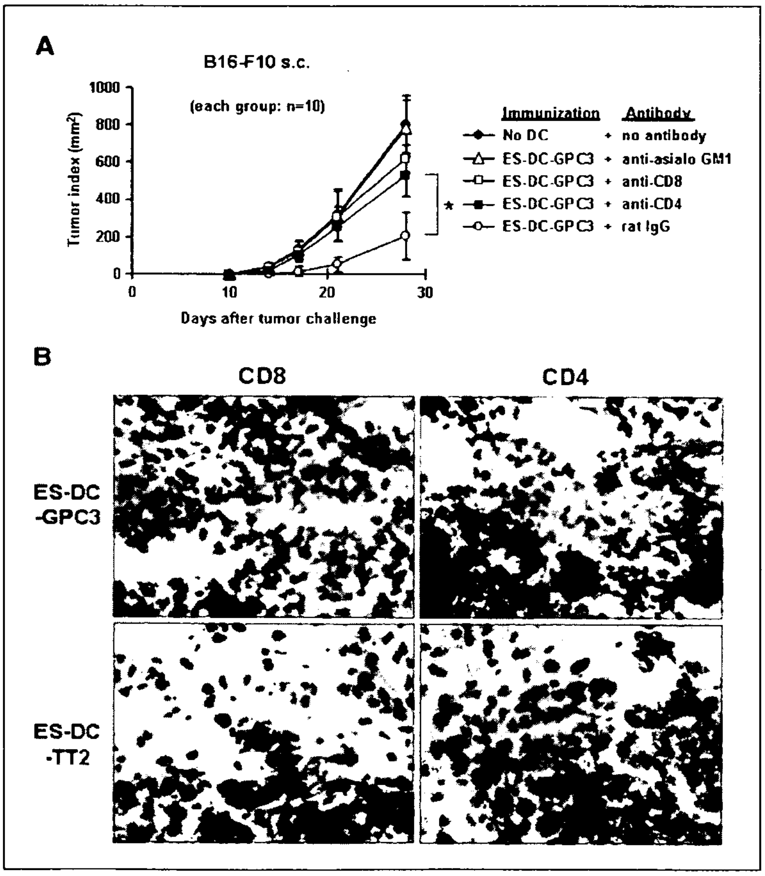

Figure 6. Involvement of both $CD4^+$ and $CD8^+$ T cells in antitumor immunity induced by ES-DC-GPC3. *A,* $CD4^+$ or $CD8^+$ T cells were depleted *in vivo* by the inoculation of anti-CD4 or anti-CD8 mAbs during immunization with ES-DC-GPC3. The mice were challenged s.c. with 5×10^3 F10 tumor cells, and the tumor size was measured and the tumor volume was represented as the tumor index. In immunization with ES-DC-GPC3, the differences in the tumor index between the mice inoculated with rat IgG and those with anti-CD4 mAb or those with anti-CD8 mAb are statistically significant (*, $P < 0.05$). The mice inoculated with anti-CD4 mAb or anti-CD8 mAb showed tumors that were the same size as those in the mice with no transfer with dendritic cells. *Points,* mean tumor index ($n = 10$ per group); *bars,* SD. *B,* infiltration of both $CD4^+$ and $CD8^+$ T cells into pulmonary metastatic tumor tissues. After the challenge with 1×10^5 F10 tumor cells as well as the pulmonary metastatic model in Fig. 5, the mice were treated twice with 1×10^5 ES-DC-TT2 or ES-DC-GPC3. Twenty days after the second treatment, frozen sections of tumor tissue were made and stained with the Giemsa method or immunostained with anti-CD4 or anti-CD8 mAb. In mice treated with ES-DC-GPC3, both $CD8^+$ and $CD4^+$ T cells apparently infiltrated into and/or around the pulmonary metastatic tumor. However, in the mice treated with ES-DC-TT2, neither $CD8^+$ nor $CD4^+$ T cells were detected in the tissue specimens. Magnification, ×400.

more immunogenic to CBF1 mice, used as the recipient mice in the present experiments, than to C57BL/6 mice. However, under the current experimental condition, all of the CBF1 mice challenged with B16-F10 or MCA-GPC3 died unless the recipient mice were treated with ES-DC-GPC3 (Fig. 4*B* and *D*), indicating that these tumor cells are invasive enough also to CBF1 mice.

In the ^{51}Cr release assay shown in Fig. 3*A* to *C*, CTL primed with ES-DC-GPC3 or ES-DC-TT2 (data not shown) exhibited weak killing activity against MCA or B16-F1 cells. Similar weak responses of spleen cells primed with ES-DC-GPC3 or ES-DC-TT2 to MCA or B16-F1 cells were also observed in the ELISPOT assay shown in Fig. 3*D*. At present, we have not yet clarified the effector cells and the target antigens that cause these "background" responses. However, such responses observed *in vitro* did not contribute to the *in vivo* antitumor effect, because the treatment with ES-DC-TT2 had no antitumor effects as shown in Fig. 4.

There was a considerable difference in the effect of treatment with ES-DC-GPC3 between the challenge with B16-F10 and that with MCA-GPC3 cells. This may be partly due to the lower expression of MHC class I on B16 compared with MCA205. B16 does not express MHC class I unless they are stimulated with IFN-γ. The indispensable role of NK cells in the antitumor effect (Fig. 6*A*) suggests that NK cells recognized B16 cells expressing a very low level of MHC class I; subsequently, NK cells produced IFN-γ to up-regulate MHC class I molecules on B16-F10 cells and to make B16-F10 cells sensitive to an attack by glypican-3-specific CTLs (35, 36).

As shown in Fig. 4, the protection against B16-F10 elicited by ES-DC-GPC3 was not complete. Treatment of the ES-DC with some maturation stimuli or loading of α-galactosylceramide, a ligand for NKT cells, to ES-DC before *in vivo* administration may have some effect to enhance the antitumor effect (37). As a future project, we are planning to generate ES-DC genetically engineered to produce cytokines, such as IL-15 or IL-21, along with glypican-3 to improve the antitumor effect.

We reported previously that the induction of immune response to glypican-3 protected the mice from a challenge with Colon 26 colon tumor cells genetically modified to overexpress glypican-3 (17). In the present study, we found the natural overexpression of glypican-3 in B16-F10 and showed that the immunization of mice with glypican-3 protected the mice from the challenge with B16-F10. Glypican-3 is one of the oncofetal proteins and the expression in normal human tissues is limited to the placenta and fetal liver (17). In addition, the tissue distribution of glypican-3 expression is very similar in mice and humans (17). As a result, our results strongly suggest that anti-melanoma and anti-hepatocellular carcinoma immunotherapy with glypican-3 seems to be an effective and safe method, and it should therefore be tested clinically.

To enable to the future clinical application of ES-DC, we recently established a method for generating ES-DC from embryonic stem cells of nonhuman primate, cynomolgus monkey, and also for genetic modification of them.[3] Considering the future clinical application of ES-DC technology, allogenicity (i.e., differences in the genetic background between the patients to be treated and the embryonic stem cells as the source for dendritic cells), we expected to cause problems. However, it is expected that human embryonic stem cells sharing some of HLA alleles with patients are available in most cases. We recently found that antigen-expressing ES-DC could potently prime antigen-specific CTL on the adoptive transfer to semiallogeneic mice, thus sharing some MHC alleles with the ES-DC and also protecting the recipient mice from subsequent challenge with tumor cells bearing the antigen (38). Immunotherapy with human ES-DC expressing glypican-3 may therefore be clinically useful as an immunotherapy of melanoma and hepatocellular carcinoma.

Acknowledgments

Received 6/15/2005; revised 11/27/2005; accepted 12/8/2005.

Grant support: Ministry of Education, Science, Technology, Sports, and Culture, Japan, grants-in-aid 12213111, 14370115, 14570421, and 14657082; Ministry of Health, Labor and Welfare, Japan, Research Grant for Intractable Diseases; Tokyo Biochemical Research Foundation; Uehara Memorial Foundation; Oncotherapy Science Co.; Eisai Pharmasential Co.; and Meiji Institute of Health Science.

The costs of publication of this article were defrayed in part by the payment of page charges. This article must therefore be hereby marked *advertisement* in accordance with 18 U.S.C. Section 1734 solely to indicate this fact.

We thank Dr. S. Aizawa (Riken Center for Developmental Biology, Kobe, Japan) for TT2, Drs. N. Takakura (Kanazawa University, Kanazawa, Japan) and T. Suda (Keio University, Tokyo, Japan) for OP9, Dr. H. Niwa (Riken Center for Developmental Biology) for pCAG-IP, and T. Kubo for technical assistance.

[3] In preparation.

References

1. O'Neill DW, Adams S, Bhardwaj N. Manipulating dendritic cell biology for the active immunotherapy of cancer. Blood 2004;104:2235–46.
2. Wen YJ, Min R, Tricot G, Barlogie B, Yi Q. Tumor lysate-specific cytotoxic T lymphocytes in multiple myeloma: promising effector cells for immunotherapy. Blood 2002;99:3280–5.
3. Asavaroengchai W, Kotera Y, Mulé JJ. Tumor lysate-pulsed dendritic cells can elicit an effective antitumor immune response during early lymphoid recovery. Proc Natl Acad Sci U S A 2002;99:931–6.
4. Zwaveling S, Ferreira Mota SC, Nouta J, et al. Established human papilloma virus type 16-expressing tumors are effectively eradicated following vaccination with long peptides. J Immunol 2002;169:350–8.
5. Prins RM, Odesa SK, Liau LM. Immunotherapeutic targeting of shared melanoma-associated antigens in a murine glioma model. Cancer Res 2003;63:8487–91.
6. Finn OJ. Cancer vaccines: between the idea and the reality. Nat Rev Immunol 2003;3:630–41.
7. Blattman JN, Greenberg PD. Cancer immunotherapy: a treatment for the masses. Science 2004;305:200–5.
8. Murphy A, Westwood JA, Teng MW, Moeller M, Darcy PK, Kershaw MH. Gene modification strategies to induce tumor immunity. Immunity 2005;22:403–14.
9. Bonehill A, Heirman C, Tuyaerts S, et al. Efficient presentation of known HLA class II-restricted MAGE-A3 epitopes by dendritic cells electroporated with messenger RNA encoding an invariant chain with genetic exchange of class II-associated invariant chain peptide. Cancer Res 2003;63:5587–94.
10. Höltl L, Ramoner R, Zelle-Rieser C, et al. Allogeneic dendritic cell vaccination against metastatic renal cell carcinoma with or without cyclophosphamide. Cancer Immunol Immunother 2005;54:663–70.
11. Erhardt M, Gorschlüter M, Sager J, et al. Transfection of human monocyte-derived dendritic cells with CpG oligonucleotides. Immunol Cell Biol 2005;83:278–85.
12. Senju S, Hirata S, Matsuyoshi H, et al. Generation and genetic modification of dendritic cells derived from mouse embryonic stem cells. Blood 2003;101:3501–8.
13. Matsuyoshi H, Senju S, Hirata S, Yoshitake Y, Uemura Y, Nishimura Y. Enhanced priming of antigen-specific CTLs *in vivo* by embryonic stem cell-derived dendritic cells expressing chemokine along with antigenic protein: application to antitumor vaccination. J Immunol 2004;172:776–86.
14. Hirata S, Senju S, Matsuyoshi H, Fukuma D, Uemura Y, Nishimura Y. Prevention of experimental autoimmune encephalomyelitis by transfer of embryonic stem cell-derived dendritic cells expressing myelin oligodendrocyte glycoprotein peptide along with TRAIL or programmed death-1 ligand. J Immunol 2005;174:1888–97.
15. Yamada A, Kawano K, Koga M, Takamori S, Nakagawa M, Itoh K. Gene and peptide analyses of newly defined lung cancer antigens recognized by HLA-A2402-restricted tumor-specific cytotoxic T lymphocytes. Cancer Res 2003;63:2829–35.
16. Monji M, Nakatsura T, Senju S, et al. Identification of a novel human cancer/testis antigen, KM-HN-1, recognized by cellular and humoral immune responses. Clin Cancer Res 2004;10:6047–57.
17. Nakatsura T, Komori H, Kubo T, et al. Mouse homologue of a novel human oncofetal antigen, glypican-3, evokes T-cell-mediated tumor rejection without autoimmune reactions in mice. Clin Cancer Res 2004;10:8630–40.
18. Oberthuer A, Hero B, Spitz R, Berthold F, Fischer M. The tumor-associated antigen PRAME is universally expressed in high-stage neuroblastoma and

associated with poor outcome. Clin Cancer Res 2004; 10:4307-13.
19. Nakatsura T, Senju S, Ito M, Nishimura Y, Itoh K. Cellular and humoral immune responses to a human pancreatic cancer antigen, coactosin-like protein, originally defined by the SEREX method. Eur J Immunol 2002;32:826-36.
20. Maraskovsky E, Sjölander S, Drane DP, et al. NY-ESO-1 protein formulated in ISCOMATRIX adjuvant is a potent anticancer vaccine inducing both humoral and CD8+ T-cell-mediated immunity and protection against NY-ESO-1+ tumors. Clin Cancer Res 2004;10: 2879-90.
21. Li B, He X, Pang X, Zhang H, Chen J, Chen W. Elicitation of both CD4 and CD8 T-cell-mediated specific immune responses to HCA587 protein by autologous dendritic cells. Scand J Immunol 2004;60:506-13.
22. Daniel D, Chiu C, Giraudo E, et al. CD4+ T cell-mediated antigen-specific immunotherapy in a mouse model of cervical cancer. Cancer Res 2005; 65:2018-25.
23. Nakatsura T, Yoshitake Y, Senju S, et al. Glypican-3, overexpressed specifically in human hepatocellular carcinoma, is a novel tumor marker. Biochem Biophys Res Commun 2003;306:16-25.
24. Capurro M, Wanless IR, Sherman M, et al. Glypican-3: a novel serum and histochemical marker for hepatocellular carcinoma. Gastroenterology 2003;125:89-97.
25. Nakatsura T, Kageshita T, Ito S, et al. Identification of glypican-3 as a novel tumor marker for melanoma. Clin Cancer Res 2004;10:6612-21.
26. Yagi T, Tokunaga T, Furuta Y, et al. A novel ES cell line, TT2, with high germline-differentiating potency. Anal Biochem 1993;214:70-6.
27. Senju S, Iyama K, Kudo H, Aizawa S, Nishimura Y. Immunocytochemical analyses and targeted gene disruption of GTPBP1. Mol Cell Biol 2000;20:6195-200.
28. Bakker J, Lin X, Nelson WG. Methyl-CpG binding domain protein 2 represses transcription from hypermethylated pi-class glutathione *S*-transferase gene promoters in hepatocellular carcinoma cells. J Biol Chem 2002;277:22573-80.
29. Niwa H, Masui S, Chambers I, Smith AG, Miyazaki J. Phenotypic complementation establishes requirements for specific POU domain and generic transactivation function of Oct-3/4 in embryonic stem cells. Mol Cell Biol 2002;22:1526-36.
30. Niwa H, Yamamura K, Miyazaki J. Efficient selection for high-expression transfectants with a novel eukaryotic vector. Gene 1991;108:193-9.
31. Nakatsura T, Senju S, Yamada K, Jotsuka T, Ogawa M, Nishimura Y. Gene cloning of immunogenic antigens overexpressed in pancreatic cancer. Biochem Biophys Res Commun 2001;281:936-44.
32. Böhm W, Thoma S, Leithäuser F, Möller P, Schirmbeck R, Reimann J. T cell-mediated, IFN-γ-facilitated rejection of murine B16 melanomas. J Immunol 1998;161:897-908.
33. Bourgault Villada I, Moyal Barracco M, Villada IB, et al. Spontaneous regression of grade 3 vulvar intraepithelial neoplasia associated with human papillomavirus-16-specific CD4+ and CD8+ T-cell responses. Cancer Res 2004;64:8761-6.
34. Fukui M, Nakano-Hashimoto T, Okano K, et al. Therapeutic effect of dendritic cells loaded with a fusion mRNA encoding tyrosinase-related protein 2 and enhanced green fluorescence protein on B16 melanoma. Tumour Biol 2004;25:252-7.
35. Xu D, Gu P, Pan PY, Li Q, Sato AI, Chen SH. NK and CD8+ T cell-mediated eradication of poorly immunogenic B16-F10 melanoma by the combined action of IL-12 gene therapy and 4-1BB costimulation. Int J Cancer 2004;109:499-506.
36. Corthay A, Skovseth DK, Lundin KU, et al. Primary antitumor immune response mediated by CD4+ T cells. Immunity 2005;22:371-83.
37. Matsuyoshi H, Hirata S, Yoshitake Y, et al. Therapeutic effect of α-galactosylceramide-loaded dendritic cells genetically engineered to express SLC/CCL21 along with tumor antigen against peritoneally disseminated tumor cells. Cancer Sci 2005;96:889-96.
38. Fukuma D, Matsuyoshi H, Hirata S, et al. Cancer prevention with semi-allogeneic ES cell-derived dendritic cells. Biochem Biophys Res Commun 2005;335:5-13.

Prevention of EAE Through Induction of Treg Cells by Transfer of ES-DC-TRAIL/MOG

S. Hirata, S. Senju, H. Matsuyoshi, D. Fukuma and Y. Nishimura

The Department of Immunogenetics, Graduate School of Medical Sciences, Kumamoto University, Kumamoto, Japan

Summary

Previously, we reported a strategy to prevent EAE by treatment of mice with genetically modified mouse ES cell-derived dendritic cells presenting MOG peptide in the context of MHC class II molecules and simultaneously expressing TRAIL or PD-L1 (ES-DC-TRAIL/MOG or -PDL1/MOG). In this study, we demonstrated that the severity of MBP-induced EAE was also reduced by ES-DC-TRAIL/MOG but not by ES-DC-PDL1/MOG. The adoptive transfer of $CD4^+CD25^+$ T cells from ES-DC-TRAIL/MOG-treated mice protected the recipient naïve mice from MOG- or MBP-induced EAE. The number of $Foxp3^+$ cells increased in the spinal cord of mice treated with ES-DC-TRAIL/MOG. These results suggest that the prevention of EAE by treatment with ES-DC-TRAIL/MOG is mediated, at least in part, by MOG-reactive $CD4^+CD25^+$ regulatory T cells.

Introduction

For the treatment of subjects with autoimmune and allergic diseases, it is desirable to down-modulate the immune response in an antigen-specific manner while not causing systemic immune suppression. In order to achieve this goal, genetically modified dendritic cells (DC) presenting target antigens and simultaneously expressing immuno-inhibitory molecules would be an attractive strategy. We also reported the protection from myelin oligodendrocyte glycoprotein (MOG)-induced experimental autoimmune encephalomyelitis (EAE) with genetically modified DC expressing MOG peptide along with TRAIL or PD-L1(1). For the genetic modification of DC, we used a method to generate DC from mouse ES cells in vitro (ES-DC) (2).

 GX15C0180

In the present study, to investigate the mechanism of the protection of MOG-induced EAE with ES-DC-TRAIL/MOG or -PDL1/MOG, we pre-treated mice with ES-DC and subjected them to EAE-induction by immunization with MBP.

Materials and Methods

Mice and cells. Male CBA and female C57BL/6 mice were mated to generate F1 (CBF1) mice, syngeneic to TT2 ES cells. The induction of differentiation of ES cells into ES-DC and generation of transfectant ES-DC, ES-DC-TRAIL, ES-DC-TRAIL/MOG and ES-DC-PDL1/MOG was done as described previously (1, 2).

Induction of EAE, treatment with ES-DC and adoptive transfer of T cells. For the induction of EAE, 6 to 8-weeks-old female CBF1 mice were immunized by a s.c. injection at the base of tail with a 0.2 ml IFA / PBS solution containing 600 μg of MOG p35-55 peptide (MEVGWYRSPFSRVVH LYRNGK), MBP p35-47 peptide(TGILDSIGRFFSG), or whole bovine MBP, and 400 μg of *M. tuberculosis* H37Ra on day 0. In addition, 500 ng of *B. pertussis* toxin were injected i.p. on days 0 and 2. For the prevention of EAE, mice were injected i.p. with ES-DC (1 x 10^6 cells/mouse/injection) on days -8, -5 and –2 (1). In some experiments, $CD25^+$ T cells were depleted by i.p. injections of anti-mouse CD25 mAb (clone PC61.5.3, 400 μg/mouse) on days -28, -24, -21, and -14. For the adoptive transfer experiments, the T cells were isolated from the spleen cells of donor mice injected with ES-DC on days -10, -7 and –4 using the MACS cell sorting system. The recipient mice were i.v. injected with the $CD4^+$, $CD4^+CD25^+$ or $CD4^+CD25^-$ T cells ($2.5x10^6$, $3x10^5$ or $2.2x10^6$ cells/mouse, respectively) on day –2, and were subjected to EAE induction on days 0 and 2. The mice were observed over a period of 42 days for clinical signs, and scores were assigned from 0 (normal) to 6 (death) (3).

Results

Prevention of MBP-induced EAE by the transfer of ES-DC-TRAIL/MOG. To investigate the mechanism for the prevention of MOG-induced EAE by the treatment of mice with ES-DC-TRAIL/MOG or -PDL1/MOG, we pre-treated mice with ES-DC and subjected them to EAE-induction by immunization with MBP (whole protein) or MBP p35-47. As shown in Fig. 1A, we found that the severity of both MBP whole protein- and peptide-induced EAE was significantly reduced by the pre-treatment with ES-DC-TRAIL/MOG. On the other hand, pre-treatment with ES-DC-PDL1/MOG, ES-DC-TRAIL/OVA (as an irrelevant antigen) and ES-DC-MOG had no effect on MBP-induced EAE (data not shown).

Prevention of MOG- and MBP-induced EAE by the adoptive transfer of $CD4^+CD25^+$ regulatory T (Treg) cells from the mice treated with ES-DC-TRAIL/MOG. We considered it is possible that MOG-reactive T cells with

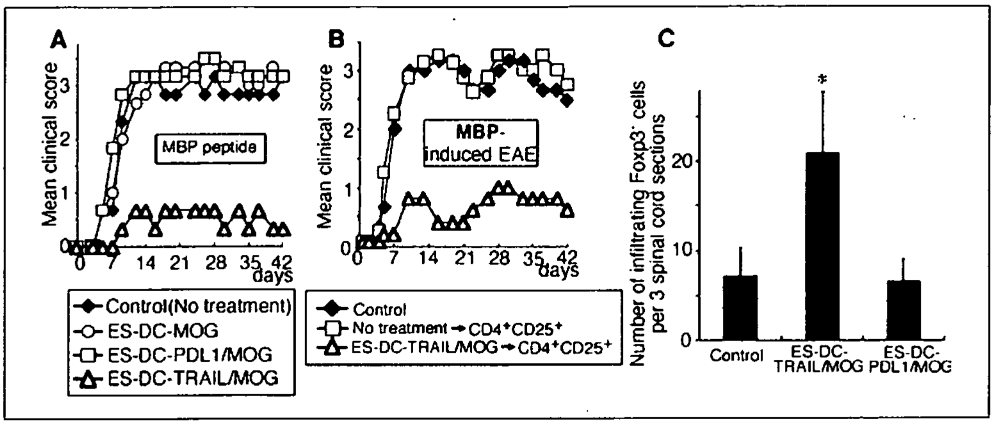

Figure 1. Prevention of MBP-induced EAE through induction of Treg cells by transfer of ES-DC-TRAIL/MOG.

immunoregulatory effect were activated or propagated by ES-DC-TRAIL/MOG to exert a protective effect against MBP-induced EAE. To address this possibility, we performed adoptive transfer experiments. As shown in Fig. 1B, the transfer of $CD4^+CD25^+$ T cells isolated from the mice treated with ES-DC-TRAIL/MOG significantly reduced the severity of not only MOG- but also MBP-induced EAE in the recipient mice. On the other hand, $CD4^+$ T cells isolated from the mice treated with ES-DC-PDL1/MOG or ES-DC-MOG, $CD4^+CD25^+$ or $CD4^+CD25^-$ T cells from the mice treated with ES-DC-TRAIL/OVA or naive mice, or $CD4^+CD25^-$ T cells from ES-DC-TRAIL/MOG-treated mice showed no effect (data not shown). Furthermore, the preventive effect of ES-DC-TRAIL/MOG on MBP-induced EAE was completely disappeared in the mice depleted in vivo of $CD4^+CD25^+$ T cells. These results support the possibility that the prevention of MBP-induced EAE by ES-DC-TRAIL/MOG was mediated by $CD4^+CD25^+$ T cells (data not shown).

Increased number of $Foxp3^+$ cells infiltrating into spinal cords of mice treated with ES-DC-TRAIL/MOG. At present, Foxp3 is the most reliable molecular marker for Treg cells. We performed immunohistochemical analysis to detect $Foxp3^+$ cells in spinal cord of mice pretreated with ES-DC and subjected to EAE induction by MOG. On day 11, the spinal cords harvested from mice were stained with anti-Foxp3 mAb and anti-CD4 mAb. As shown in Fig. 1C, the infiltration of $Foxp3^+$ cells into the spinal cord was enhanced in mice treated with ES-DC-TRAIL/MOG, compared with mice with no treatment or mice treated with ES-DC-PDL1/MOG. These results further support the notion of involvement of Treg cells in the disease-protection effect.

Conclusion

It may be possible that the prevention of EAE by treatment with ES-DC-

TRAIL/MOG is mediated, at least in part, by MOG-reactive $CD4^+CD25^+$ Treg cells activated by ES-DC-TRAIL/MOG (3).

References

1. Hirata, S., Senju, S., Matsuyoshi, H., et al. Prevention of experimental autoimmune encephalomyelitis by transfer of embryonic stem cell-derived dendritic cells expressing myelin oligodendrocyte glycoprotein peptide along with TRAIL or programmed death-1 ligand. J Immunol, *174:* 1888-1897, 2005.
2. Senju, S., Hirata, S., Matsuyoshi, H., et al. Generation and genetic modification of dendritic cells derived from mouse embryonic stem cells. Blood, *101:* 3501-3508, 2003.
3. Hirata, S., Matsuyoshi, H., Fukuma, D., et al. Involvement of regulatory T cells in the experimental autoimmune encephalo-myelitis-preventive effect of dendritic cells expressing myelin oligodendrocyte glycoprotein plus TRAIL. J Immunol, *in press*

Prevention of Experimental Autoimmune Encephalomyelitis by Transfer of Embryonic Stem Cell-Derived Dendritic Cells Expressing Myelin Oligodendrocyte Glycoprotein Peptide along with TRAIL or Programmed Death-1 Ligand[1]

Shinya Hirata, Satoru Senju, Hidetake Matsuyoshi, Daiki Fukuma, Yasushi Uemura, and Yasuharu Nishimura[2]

Experimental autoimmune encephalomyelitis (EAE) is caused by activation of myelin Ag-reactive CD4$^+$ T cells. In the current study, we tested a strategy to prevent EAE by pretreatment of mice with genetically modified dendritic cells (DC) presenting myelin oligodendrocyte glycoprotein (MOG) peptide in the context of MHC class II molecules and simultaneously expressing TRAIL or Programmed Death-1 ligand (PD-L1). For genetic modification of DC, we used a recently established method to generate DC from mouse embryonic stem cells (ES cells) in vitro (ES-DC). ES cells were sequentially transfected with an expression vector for TRAIL or PD-L1 and an MHC class II-associated invariant chain-based MOG epitope-presenting vector. Subsequently, double-transfectant ES cell clones were induced to differentiate to ES-DC, which expressed the products of introduced genes. Treatment of mice with either of the double-transfectant ES-DC significantly reduced T cell response to MOG, cell infiltration into spinal cord, and the severity of MOG peptide-induced EAE. In contrast, treatment with ES-DC expressing MOG alone, irrelevant Ag (OVA) plus TRAIL, or OVA plus PD-L1, or coinjection with ES-DC expressing MOG plus ES-DC-expressing TRAIL or PD-L1 had no effect in reducing the disease severity. In contrast, immune response to irrelevant exogenous Ag (keyhole limpet hemocyanin) was not impaired by treatment with any of the genetically modified ES-DC. The double-transfectant ES-DC presenting Ag and simultaneously expressing immune-suppressive molecules may well prove to be an effective therapy for autoimmune diseases without inhibition of the immune response to irrelevant Ag. *The Journal of Immunology,* **2005, 174: 1888–1897.**

Currently, corticosteroids and other immune suppressants are commonly used for treatment of subjects with autoimmune diseases. The medication with these drugs often leads to systemic immune suppression and consequent opportunistic infections. Thus, it is desirable to develop a therapeutic means to down-modulate immune responses in an Ag-specific manner without causing systemic immune suppression.

Experimental autoimmune encephalomyelitis (EAE),[3] an animal model for human multiple sclerosis, is characterized by neurological impairment resulting from demyelination in the CNS caused by myelin Ag-reactive CD4$^+$ T cells. This disease model is induced by immunization with myelin Ags such as myelin oligodendrocyte glycoprotein (MOG). In the current study, we wanted to try to prevent MOG-induced EAE by treatment of mice with genetically modified dendritic cells (DC). We generated double-transfectant DC presenting MOG peptide in the context of MHC class II molecules and simultaneously expressing molecules with T cell-suppressive property. We tested a strategy to down-modulate the immune response in an Ag-specific manner by in vivo transfer of such genetically modified DC to prevent development of the disease.

For efficient presentation of MOG peptide in the context of MHC class II molecules, we used a previously devised expression vector in which cDNA for human MHC class II-associated invariant chain (Ii) was mutated to contain antigenic peptide in the class II-associated Ii peptide (CLIP) region (1). An epitope inserted in this vector is efficiently presented in the context of coexpressed MHC class II molecules (2). Because they are molecules with a T cell-suppressive property, we tested TRAIL and Programmed Death-1 ligand (PD-L1). TRAIL, a member of the TNF superfamily, is constitutively expressed in a variety of cell types, including lymphocytes, NK cells, and neural cells (3, 4). TRAIL$^{-/-}$ mice are hypersensitive to collagen-induced arthritis and streptozotocin-induced diabetes (5). PD-L1, a ligand for PD-1 and member of the CD28/CTLA-4 family, is expressed on DC, IFN-γ-treated monocytes, activated T cells, placental trophoblasts, myocardial endothelium, and cortical thymic epithelial cells (6, 7). PD-1$^{-/-}$ mice spontaneously develop a lymphoproliferative/autoimmune disease, a lupus-like disease, arthritis, and cardiomyopathy (8, 9). Thus, abrogation of either of these two molecules make mice autoimmune prone, suggesting that these molecules play significant roles

Department of Immunogenetics, Graduate School of Medical Sciences, Kumamoto University, Kumamoto, Japan

Received for publication May 20, 2004. Accepted for publication December 8, 2004.

The costs of publication of this article were defrayed in part by the payment of page charges. This article must therefore be hereby marked *advertisement* in accordance with 18 U.S.C. Section 1734 solely to indicate this fact.

[1] This work was supported in part by Grants-in-Aid 12213111, 14370115, 14570421, and 14657082 from the Ministry of Education, Science, Technology, Sports, and Culture, Japan, and a Research Grant for Intractable Diseases from Ministry of Health, Labour and Welfare, Japan, and grants from the Tokyo Biochemical Research Foundation and Uehara Memorial Foundation, and by funding from Meiji Institute of Health Science.

[2] Address correspondence and reprint requests to Dr. Yasuharu Nishimura, Department of Immunogenetics, Graduate School of Medical Sciences, Kumamoto University, Honjo 1-1-1, Kumamoto 860-8556, Japan. E-mail address: mxnishim@gpo.kumamoto-u.ac.jp

[3] Abbreviations used in this paper: EAE, experimental autoimmune encephalomyelitis; MOG, myelin oligodendrocyte glycoprotein; DC, dendritic cell; Ii, invariant chain; CLIP, class II-associated Ii peptide; PD-L1, Programmed Death-1 ligand; ES cell, embryonic stem cell; ES-DC, ES cell-derived DC; PLP, myelin proteolipid protein; MBP, myelin basic protein; IRES, internal ribosomal entry site; PCC, pigeon cytochrome *c*; KLH, keyhole limpet hemocyanin.

0022-1767/05/$02.00